Yang *et al.*
Chinese Journal of Mechanical Engineering (2024) 37:16
https://doi.org/10.1186/s10033-024-01001-z

Chinese Journal of Mechanical Engineering

ORIGINAL ARTICLE

Open Access

On the Polygonal Wear Evolution of Heavy-Haul Locomotive Wheels due to Wheel/Rail Flexibility and Its Mitigation Measures

Yunfan Yang[1,2], Feifan Chai[2], Pengfei Liu[1], Liang Ling[2], Kaiyun Wang[2] and Wanming Zhai[2*]

Abstract

Wheel polygonal wear can immensely worsen wheel/rail interactions and vibration performances of the train and track, and ultimately, lead to the shortening of service life of railway components. At present, wheel/rail medium- or high-frequency frictional interactions are perceived as an essential reason of the high-order polygonal wear of railway wheels, which are potentially resulted by the flexible deformations of the train/track system or other external excitations. In this work, the effect of wheel/rail flexibility on polygonal wear evolution of heavy-haul locomotive wheels is explored with aid of the long-term wheel polygonal wear evolution simulations, in which different flexible modeling of the heavy-haul wheel/rail coupled system is implemented. Further, the mitigation measures for the polygonal wear of heavy-haul locomotive wheels are discussed. The results point out that the evolution of polygonal wear of heavy-haul locomotive wheels can be veritably simulated with consideration of the flexible effect of both wheelset and rails. Execution of mixed-line operation of heavy-haul trains and application of multi-cut wheel re-profiling can effectively reduce the development of wheel polygonal wear. This research can provide a deep-going understanding of polygonal wear evolution mechanism of heavy-haul locomotive wheels and its mitigation measures.

Keywords Heavy-haul locomotive, Wheel polygonal wear, Wheel/rail flexibility, Long-term polygonal wear evolution, Mitigation measures

1 Introduction

1.1 Engineering Background

Polygonal wear is a prevalent phenomenon that generates around the circumference of railway wheels, which is probed on-board and can degenerate wheel/rail contact, vibration and fatigue mechanics performances of railway key components, braking ability and ambient noise [1–5]. Currently, the ever-increasing traction power and axle load of heavy-haul trains and rapidly deteriorated service conditions (such as the inconstant meteorological conditions, complex curve laying, varying adhesion status, long steep, line settlement) can degenerate wheel/rail adhesion-slip interactions to a large extent, and accelerate the development of the high-order polygonal wear of railway wheels (see Figure 1).

Wheel polygonal wear breeds generally not only on the high-speed and metro trains, but also on the heavy-haul locomotives all around the world [1, 6]. In China, the 16th–25th order polygonization dominates on locomotive wheels, which can result in the destructive vibrations with the frequency range of 70–130 Hz and persistently touch off the abnormal vibration alarm system (AVAS) [7, 8]. More seriously,

*Correspondence:
Wanming Zhai
wmzhai@swjtu.edu.cn
Full list of author information is available at the end of the article

© The Author(s) 2024. **Open Access** This article is licensed under a Creative Commons Attribution 4.0 International License, which permits use, sharing, adaptation, distribution and reproduction in any medium or format, as long as you give appropriate credit to the original author(s) and the source, provide a link to the Creative Commons licence, and indicate if changes were made. The images or other third party material in this article are included in the article's Creative Commons licence, unless indicated otherwise in a credit line to the material. If material is not included in the article's Creative Commons licence and your intended use is not permitted by statutory regulation or exceeds the permitted use, you will need to obtain permission directly from the copyright holder. To view a copy of this licence, visit http://creativecommons.org/licenses/by/4.0/.

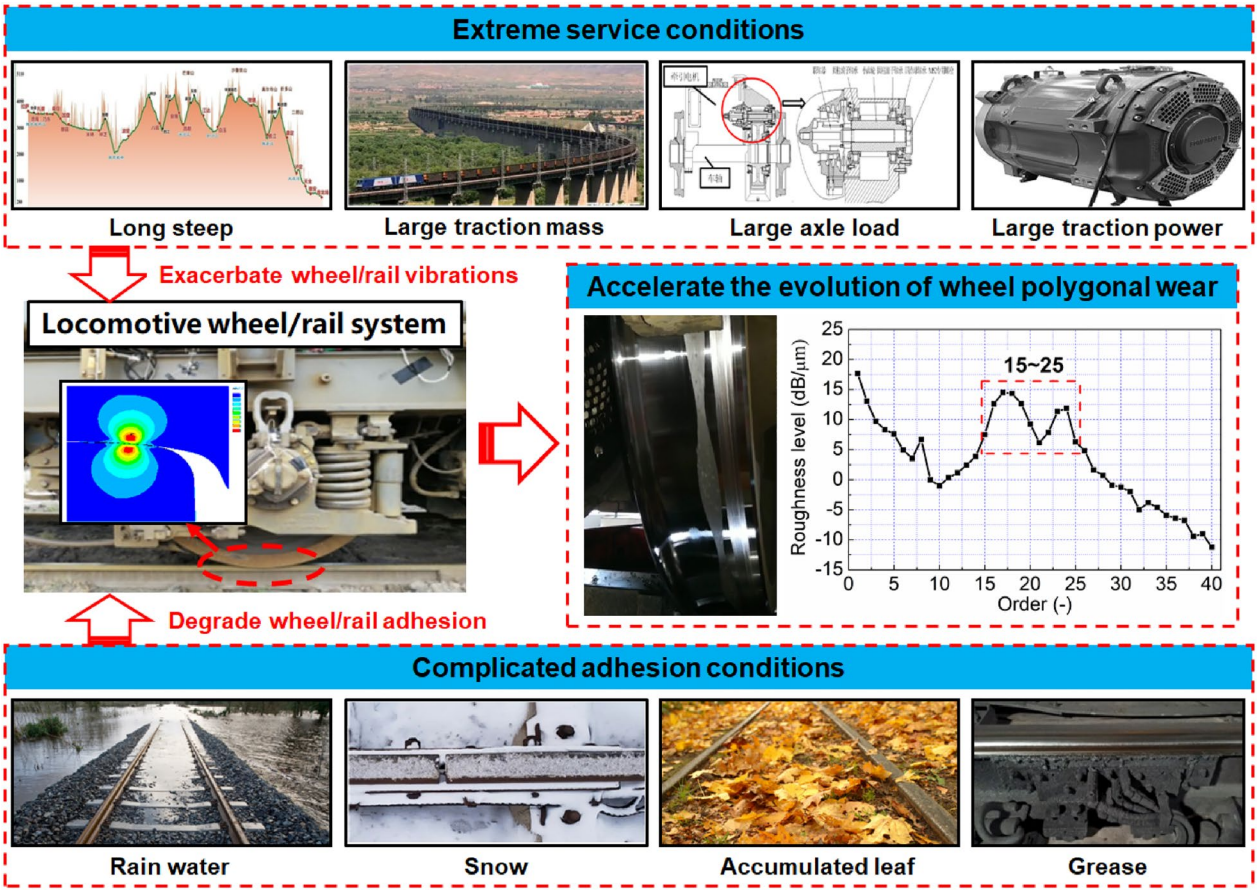

Figure 1 Aggravation of polygonal wear of heavy-haul locomotive wheels due to the extreme service conditions and complicated wheel/rail adhesion statuses

the high-order wheel polygonal wear can cause the failure fracture of locomotive parts (such as the cracks appearing on the wheel rim, steel spring, oil damper, gearbox housing, gear pair) [6]. Wheel re-profiling is the most common and immediate way to remove the wear damage on the wheel tread, which nevertheless, can't eradicate the initiation of high-order wheel polygonal wear and will immensely reduce the using life of locomotive wheelsets. Thus, it is meaningful to understand the polygonal wear evolution of locomotive wheels and come up with the effective countermeasures.

1.2 Review of Related Researches

Wheel polygonal wear is an ongoing concern which has not been eradicated till now. Therefore, substantial funds have been invested and special research projects have been established with the pressing aim to settle the wheel polygonal wear problem all around the world. Meanwhile, many publications reported wheel polygonal wear, among which the formation mechanism of wheel polygonal wear has always been most principally focused.

1.2.1 On the Formation Mechanism of Wheel Polygonal Wear

The formation mechanism of polygonal wear of high-speed, metro and locomotive wheels with different wavelength has been followed with great interest, which however, is still a moot point. At present, the coupled resonance of the train-track system has been most extensively acknowledged as the formation mechanism of high-order polygonal wear of railway wheels (namely, the so-called "fixing-frequency mechanism") [9].

In China, the noteworthy polygonal wear issues of high-speed wheels have aroused researchers' attention since 2008, and the prominent order of which are 18th–26th that can procreate the excitation frequency of 500–630 Hz [6, 10]. Based on the polygonal wear

evolution simulations, on-line vibration tests, modal tests and full-size wheel/rail rolling tests, the resonance modes of the bogie [11, 12], rail local bending mode between two wheelsets of the same bogie [10, 13, 14] and wheel/rail frictional self-excited vibrations [15, 16] are indicated to be the fundamental cause of the high-order polygonal wear of high-speed wheels. On the other hand, the 5th–8th, 8th–9th, 11th–16th and 12th–14th order polygonal wear are reported appearing on the metro wheels with different vehicle architectonics and running speeds [6, 17–20]. The low-order bending mode of the wheelset [17, 18], P2 resonance [19], and residuary 4th order wheel polygonal wear after wheel re-profiling are proved to be the root cause of the polygonal wear of metro wheels.

The heavy-haul locomotives encounter much harsher operation conditions in comparison to the high-speed and metro trains, which accordingly makes their wheel/rail frictional contact and wheel polygonal wear problems more serious. In South Africa, a fair number of locomotive wheels suffer from 20th order polygonal wear with relatively high wear amplitudes (higher than 0.2 mm). Fröhling and Spangenberg et al. [21, 22] stated that the torsional vibrations of the wheelset which caused by the wheel/rail self-excited stick-slip vibrations under saturated adhesion conditions and along with the harmonics and interharmonics components released from the AC traction motor contribute to the formation of the 20th order polygonal wear. In China, 17th–19th and 23rd–25th order polygonal wear can be found in certain types of locomotives (see Figure 1), which cause the abnormal vibrations with the passing frequency of 80–130 Hz and develop rapidly after poor-quality re-profiling [7, 8]. Tao et al. [23, 24] stated that the first bending mode of the wheelset (with the modal frequency of 84 Hz) and lateral bending mode of wheel disc (with the modal frequency of 122 Hz) could result in the corresponding tangential interactions between the wheels and rails, and consequently, brought into the existence of 17th–19th and 23rd–25th order wheel polygonal wear. Furthermore, Refs. [24, 25] pointed out that the wheel discrete circumferential defect could excite the flexible deformations of the wheelset and oscillations in wheel/rail frictional contact and expedite the development of the high-order polygonization of locomotive wheels. On the other hand, Peng et al. [26] stated that the low-order bending modes and umbrella mode of the wheelset could contribute to the development of the polygonization of locomotive wheels only when they were excited and the according oscillations wheel/rail lateral creepage was dominated.

1.2.2 On the Countermeasure of Wheel Polygonal Wear

Feasible countermeasures against the polygonal wear of railway wheels can effectively ease the abnormal vibration and fatigue fracture accidents. At present, wheel re-profiling has been the most common way to clear the surface wear damage of wheel tread, which however, is palliative. According to the on-site observations, the high-order polygonal wear of locomotive wheels still has residue and achieve an obvious development due to the unsound re-profiling works. The levels of high-order wheel polygonal wear with less than a month of operation after re-profiling even reached that before re-profiling [7, 8]. To address this issue, Cui et al. [27] suggested that adopting two cuts when re-profiling and appropriately adjusting the space between the two friction rollers of wheel lathe could significantly reduce the roughness levels of high-order wheel polygonal wear. Refs. [7, 28] prove that improving the quality of re-profiling by strengthening the fixation of wheelset can avoid the residue of the high-order polygonal wear of locomotive wheels. Moreover, the authors pointed out that the high-order polygonal wear of locomotive wheels can be thoroughly removed by the wheel lathe after disassembling the wheels from the locomotive and develops slowly after re-profiling, which nevertheless, is much more time-consuming than that by using the under-floor wheel lathe [7].

Wheel/rail wear damage is directly affected by the frictional contact. Hence, some scholars put forward that the evolution of wheel polygonal wear can be relieved via controlling the level of wheel/rail excitations and frictional interactions. Reducing the traction loading and wheel/rail adhesion levels [18], controlling the roughness level of track irregularities [19], dampening the bending vibrations of the rail between two wheelsets and wheel/rail interactions by increasing the damping of railpads [29, 30], and decreasing wheel/rail slipping rate by regulating the control threshold of the anti-slip controller [31] are capable of restraining the development of high-order wheel polygonal wear. On the other hand, on account of the viewpoint that the formation of high-order wheel polygonal wear is directly related to the flexible deformations of the wheelset, the structural design of the wheelset is proposed to be appropriately adjusted to refrain from the initiation of high-order polygonal wear. Given this, Wen's research group suggested that the stiffness of the wheelset can be enhanced and the bending vibrations can correspondingly be suppressed by marginally thickening the wheel web or increasing the diameter of the wheelset axle [28]. As in the following, the wheel/rail lateral creep forces, frictional wear and the resulting development of high-order polygonal wear can be tellingly refrained.

Furthermore, altering the speed where the variable frequency drive (VFD) pulse mode changed [32], adjustment of the travelling velocity of the train [11, 20], and improving the hardness ratio of wheel to rail materials [33] are also mentioned to have possibility to slow down the increase of the wheel polygonal wear.

To sum up, the countermeasures against the wheel polygonal wear mainly involve the following aspects:

- Improving the quality of wheel re-profiling.
- Controlling the level of wheel/rail dynamic interactions.
- Ameliorating the structure and parameter design of train-track system.
- Others.

1.3 Motivations and Contributions of This Study

The essential features of wheel polygonal wear of railway trains are quite complicated and various in light of the non-determinacies and diversities existing in the traveling velocity, service statuses, structural design of train and track, braking modes, etc. Till now, the "fixing-frequency mechanism" has been often employed to determine the formation mechanism of polygonal wear of railway wheels. However, the sources of the concerned resonance excitation and how to identify their impact on the evolution of the wheel polygonal wear are still controversial. On the other hand, the need of countermeasures against the wheel polygonal wear is urgent regarding its menace on the traveling quality. However, some aforementioned countermeasures are roughly proposed and short of systematic verifications.

In this research work, a long-term wheel polygonal wear evolution model with consideration of different flexible modeling of the wheel/rail coupled system is established. The effect of wheel/rail flexible vibrations on wheel/rail frictional interactions and polygonal wear evolution of the heavy-haul locomotive wheels is researched, which has been rarely discussed in the past. Furthermore, two countermeasures for the polygonal wear of locomotive wheels are experimentally investigated, and the feasibility and effectiveness of which are carefully discussed through field investigations.

2 Methodology

2.1 Technical Route

The long-term wheel wear prediction model has been popularly used to reproduce the evolution of polygonal wear of railway wheels [34, 35]. Here, a long-term wheel polygonal wear prediction model is performed in this study, where the following major parts are contained (see Figure 2): (i) Heavy-haul train-track coupled dynamics model with consideration of different flexible modeling of wheel/rail system; (ii) Polygonal wear evolution prediction model on account of the wheel/rail non-Hertzian contact and USFD wear function [31, 36]; (iii) Post-processing (including smoothing and amplification processes) and updating of wheel polygonal wear.

The calculation flow of polygonal wear evolution is illustrated in Figure 2 and can be summarized as follows [31, 34, 35]:

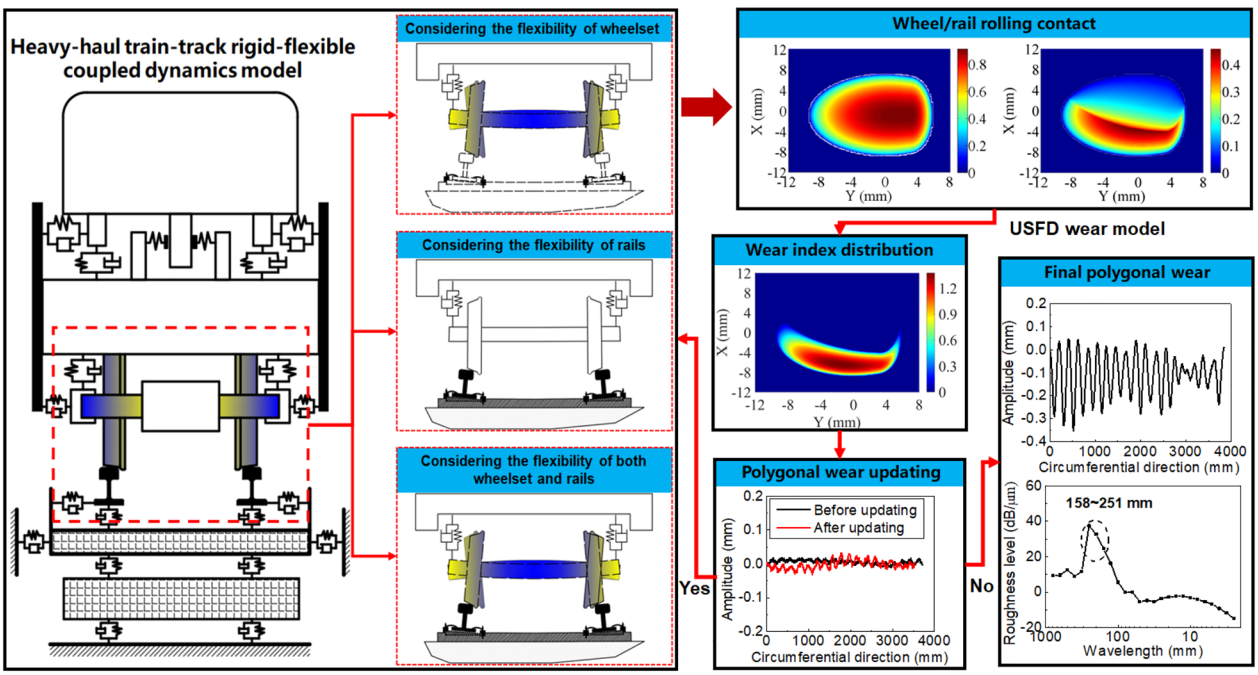

Figure 2 Calculation flow of wheel polygonal wear prediction

- Step 1: Input the initial wheel polygonal wear, and along with the designing and controlling parameters of the train-track coupled system.
- Step 2: Respectively run the train-track non-linear dynamics model involving different flexible modeling of the wheel/rail coupled system (including Model-I, -II, and -III), and acquire the non-Hertzian distributions of the wheel/rail stress and local relative slipping.
- Step 3: Obtain the wear distributions based on USFD wear function and non-Hertzian contact analysis.
- Step 4: Calculate the wear depth at the discrete points around the circumference of the wheel based on wear distributions, and obtain the accumulative polygonal wear after each iteration calculation.
- Step 5: Appropriately smooth and amplify the obtained polygonal wear, and feedback it back to the dynamics model while the iteration calculation is cycled (Step 2). Otherwise output the final wheel polygonal wear.

To enhance the computing efficiency, the polygonal wear is assumed to be concentrated on the normal rolling circle of the wheel since the differences of polygonal wear at different locations along the wheel tread are small. Furthermore, the wheel/rail profiles and wheel perimeter are set to be unchanged and unaffected by the frictional wear.

2.2 Train-Track Rigid-Flexible Coupled Dynamics Model

The high-order polygonal wear of railway wheels is widely acknowledged to be subjected to the medium- and high-frequency wheel/rail coupled resonances which are mainly resulted by the flexible deformations of the wheelset and rail. In this study, a heavy-haul train-track rigid-flexible coupled dynamics model with consideration of different flexible modeling of wheel/rail system is extended based on the basic principle of vehicle-track coupled dynamics [37, 38], where the following three wheel/rail flexible modeling scenarios are involved (see Figure 3):

- ***Model-I*** With only consideration of flexibility of locomotive wheelset, and the vibrations of the ballast track are solved by the lumped-parameter model where the rails are modeled as the rigid bodies. In this model, the medium- and high-frequency wheel/rail frictional contact and wear are mainly caused by the flexible vibrations of the wheelset.

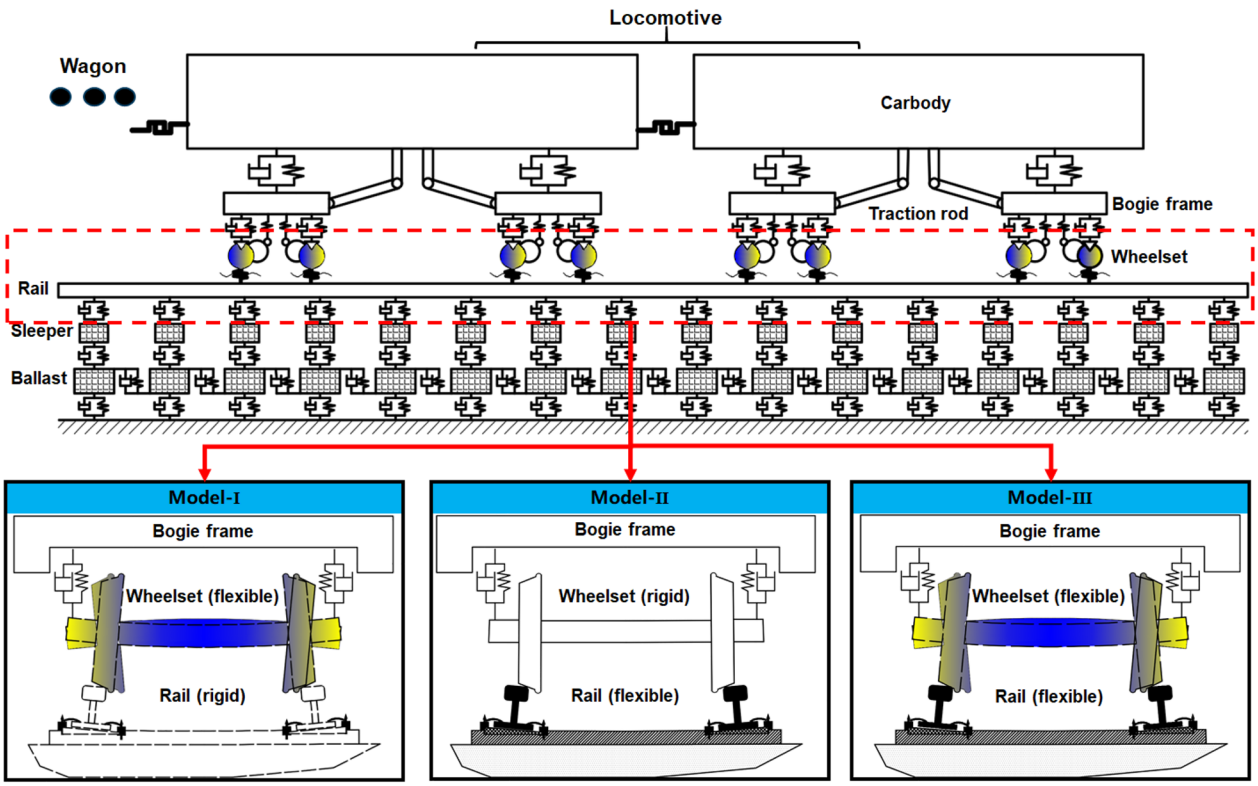

Figure 3 Heavy-haul train-track rigid-flexible coupled dynamics model with consideration of different flexible modeling of wheel/rail system

- ***Model-II*** With only consideration of flexibility of the rails, and the flexibility of locomotive wheelset is ignored. In this model, the medium- and high-frequency wheel/rail frictional contact and wear are mainly caused by the flexible vibrations of the rails.
- ***Model-III*** With both consideration of flexibility of the locomotive wheelset and rails. In this model, the medium- and high-frequency wheel/rail frictional contact and wear are caused by the flexible coupled vibrations of both wheelset and rails.

2.2.1 Train Sub-model

Hereon, the heavy-haul train is constituted by two locomotives and a series of wagons, in which the spatial vibrations of locomotives are focused and modeled in detailed, and the one-dimensional single-mass model is employed to simulate the longitudinal motion of the wagons. The locomotive model comprises a carbody, two bogie frames, two traction rods, four traction motors and four wheelsets, which are connected by primary and secondary suspension elements. The suspension components are modeled by the spring-damping elements. Furthermore, all locomotive components except for the wheelsets are treated as rigid bodies with consideration of all six degrees of freedom (DOFs).

Special attentions are paid to uncover the influence of the flexibility of locomotive wheelsets on polygonal wear evolution in this work. In view of this, the locomotive wheelsets are modeled with consideration of flexibility in Model-I and Model-III, whereas they are regarded as rigid bodies in Model-II. The flexible vibrations of locomotive wheelset can be obtained by modal superposition method [25, 31]. In this work, the first twelve flexible modes of locomotive wheelset with respect to the natural frequency range of 0–434 Hz that extracted from commercial software ANSYS are focused. The first bending mode of the wheelset (with the mode frequency of 81.0 Hz) and lateral bending mode of wheel disc (with the mode frequency of 132.5 Hz) are exhibited in Figure 4, which are very close to the excitation frequency of 17th–25th order polygonal wear of locomotive wheels, and elaborated to be the root cause of its initiations by Tao et al. [23, 24]. The rest of the locomotive wheelset mode shapes can be referred in Ref. [39]. Furthermore, the rotation effect of the flexible wheelset is not considered and numerically modelled in this paper since the non-linear vibration (bifurcation) phenomena caused by which with a relatively low traveling speed are not significant [40, 41].

The non-linear vibration equation for the heavy-haul train sub-model can be given as [37]

$$\boldsymbol{M}_{\mathbf{HT}}^{(\mathrm{C})}\ddot{\boldsymbol{x}}_{\mathbf{HT}}^{(\mathrm{C})}+\boldsymbol{C}_{\mathbf{HT}}^{(\mathrm{C})}\dot{\boldsymbol{x}}_{\mathbf{HT}}^{(\mathrm{C})}+\boldsymbol{K}_{\mathbf{HT}}^{(\mathrm{C})}\boldsymbol{x}_{\mathbf{HT}}^{(\mathrm{C})}=-\boldsymbol{F}_{\mathbf{wr}}. \tag{1}$$

The symbols $\boldsymbol{M}_{\mathbf{HT}}^{(\mathrm{C})}$, $\boldsymbol{C}_{\mathbf{HT}}^{(\mathrm{C})}$ and $\boldsymbol{K}_{\mathbf{HT}}^{(\mathrm{C})}$ represent the mass, damping and stiffness matrixes of the train sub-model respectively, where the superscript "(C)" stands for the built models including Model-I, Model-II and Model-III. $\boldsymbol{x}_{\mathbf{HT}}^{(\mathrm{C})}$, $\dot{\boldsymbol{x}}_{\mathbf{HT}}^{(\mathrm{C})}$ and $\ddot{\boldsymbol{x}}_{\mathbf{HT}}^{(\mathrm{C})}$ denote the displacement, velocity and acceleration vectors of the train sub-model, respectively. $\boldsymbol{F}_{\mathbf{wr}}$ is the wheel/rail interaction vector.

2.2.2 Track Sub-model

The influence of flexible deformations of the ballast track, especially the rails, on the polygonal wear evolution of the locomotive wheels is followed with interest in this study. Hereon, the ballast track is modeled as a lumped-parameter model in Model-I, and which inversely, is modeled as a layered model taking the high-frequency responses of rails into account in Model-II and Model-III. In Model-II and Model-III, the lateral and vertical bending vibrations of the rails are calculated by the simply supported Euler-Bernoulli beam model, and longitudinal and torsional vibrations of the rails are solved by the rod model with consideration of fixed-constraint at both ends. Also, the flexible responses of the rails are obtained by modal superposition method [2, 37]. The vibration equations of the rail can be expressed as:

$$\begin{cases} m_r\frac{\partial^2 X_r(x,t)}{\partial t^2}-E_rA_r\frac{\partial^2 X_r(x,t)}{\partial x^2}=-\sum\limits_{i=1}^{N_s}F_{sxi}(t)\delta(x-x_{si})-\sum\limits_{k=1}^{N_c}\sum\limits_{j=1}^{N_w}F_{wrxi}(t)\delta\left(x-x_{w(k,j)}\right), \\ E_rI_{rz}\frac{\partial^4 Y_r(x,t)}{\partial x^4}+m_r\frac{\partial^2 Y_r(x,t)}{\partial t^2}=-\sum\limits_{i=1}^{N_s}F_{syi}(t)\delta(x-x_{si})+\sum\limits_{k=1}^{N_c}\sum\limits_{j=1}^{N_w}F_{wryi}(t)\delta\left(x-x_{w(k,j)}\right), \\ E_rI_{ry}\frac{\partial^4 Z_r(x,t)}{\partial x^4}+m_r\frac{\partial^2 Z_r(x,t)}{\partial t^2}=-\sum\limits_{i=1}^{N_s}F_{szi}(t)\delta(x-x_{si})+\sum\limits_{k=1}^{N_c}\sum\limits_{j=1}^{N_w}F_{wrzi}(t)\delta\left(x-x_{w(k,j)}\right), \\ \rho_rI_{r0}\frac{\partial^2\phi_r(x,t)}{\partial t^2}-G_rI_t\frac{\partial^2\phi_r(x,t)}{\partial x^2}=-\sum\limits_{i=1}^{N_s}M_{si}(t)\delta(x-x_{si})+\sum\limits_{k=1}^{N_c}\sum\limits_{j=1}^{N_w}M_{wri}(t)\delta\left(x-x_{w(k,j)}\right). \end{cases} \tag{2}$$

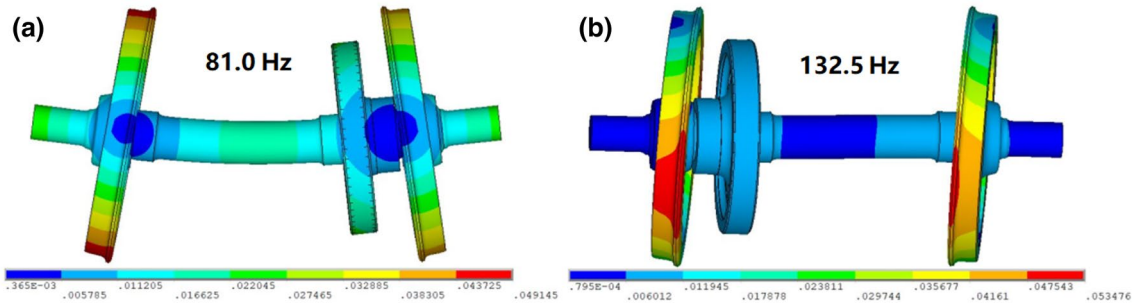

Figure 4 Eigen-mode of the locomotive wheelset: (**a**) First bending mode of the wheelset (81.0 Hz) and (**b**) lateral bending mode of wheel disc (132.5 Hz)

The symbols employed in the above formula can be referred in Ref. [37]. Further, these partial differential equations can be converted to second-order ordinary differential equations by applying the Ritz method. The according derivation procedures of the vibrations of the rail can be referred in Ref. [37] and are omitted hereon.

Moreover, the sleepers and ballast are simplified as rigid bodies in all established models, and the rail fastenings and connections between the sleepers and ballast are modeled as spring-damper elements. The deformations of the subgrade are disregarded due to their negligible impact on wheel/rail interactions and polygonal wear evolution of locomotive wheels.

The non-linear vibration equation for the ballast track sub-model can be given as [37]

$$\boldsymbol{M}_{\mathrm{BT}}^{(\mathrm{C})}\ddot{\boldsymbol{x}}_{\mathrm{BT}}^{(\mathrm{C})}+\boldsymbol{C}_{\mathrm{BT}}^{(\mathrm{C})}\dot{\boldsymbol{x}}_{\mathrm{BT}}^{(\mathrm{C})}+\boldsymbol{K}_{\mathrm{BT}}^{(\mathrm{C})}\boldsymbol{x}_{\mathrm{BT}}^{(\mathrm{C})}=\boldsymbol{F}_{\mathrm{wr}}. \tag{3}$$

2.2.3 Wheel/Rail Interaction Sub-model

Wheel/rail non-linear interaction sub-model that concatenates the train sub-model and the track sub-model primarily covers the calculations of spatial contact geometry and normal and tangential contact, which has a significant effect on solving the wheel/rail frictional contact and wheel wear evolutions. In this research, the influence of wheel/rail flexible deformations on wheel/rail contact, especially on the spatial contact geometry, normal elastic compression as well as wheel/rail creep, is carefully treated.

Wheel/rail vertical relative displacement with consideration of the flexible deformations of the wheelset can be expressed as

$$\begin{aligned}\delta_{\mathrm{wr(L,R)}i}(t)=&Z_{\mathrm{w}i}(t)+u_{\mathrm{fwz(L,R)}i}(t)\\&-\left(Z_{\mathrm{wr(L,R)}i}(t)-\delta_{\mathrm{wr0}}\right),\end{aligned} \tag{4}$$

where t is the operating time. $Z_{\mathrm{w}i}(t)$ denotes the vertical displacement of the ith wheelset. $Z_{\mathrm{wr(L,R)}i}(t)$ denotes the minimum vertical distances from the left and right wheels to the rails, and δ_{wr0} denotes the minimum vertical distances at the initial moment. $u_{\mathrm{fwz(L,R)}i}(t)$ denotes the flexible deformation of the left and right wheel centers.

On the other hand, the wheel/rail contact geometry and creepage which contribute greatly to the wheel/rail frictional contact and wear damage are highly influenced by the vibrations of the wheel tread. The wheel/rail creepage can be expressed as

$$\vartheta_{(x,y,\phi)}^{(\mathrm{C})}=\frac{\Delta\boldsymbol{\nu}_{\mathrm{wr}(x,y,\phi)}^{(\mathrm{C})}}{\nu_{\mathrm{w}}}=\frac{\boldsymbol{A}^{(\mathrm{C})}\left(\dot{\boldsymbol{u}}_{\mathrm{w}(x,y,\phi)}^{(\mathrm{A})}-\dot{\boldsymbol{u}}_{\mathrm{r}(x,y,\phi)}^{(\mathrm{A})}\right)}{\nu_{\mathrm{w}}}, \tag{5}$$

with the spatial vibrations of the wheel tread considering the wheelset flexibility deduced as

$$\begin{aligned}\dot{\boldsymbol{u}}_{\mathrm{w}(x,y,\phi)}^{(\mathrm{A})}&=\dot{\boldsymbol{u}}_{\mathrm{R}(x,y,\phi)}^{(\mathrm{A})}+\dot{\boldsymbol{u}}_{\mathrm{con}(x,y,\phi)}^{\mathrm{F}}\\&=\dot{\boldsymbol{u}}_{\mathrm{R}(x,y,\phi)}^{(\mathrm{A})}+\sum_{k=1}^{N_{\mathrm{fw}}}\boldsymbol{\Psi}_{\mathrm{fw}k}(\boldsymbol{x}_{\mathrm{con}})\dot{\boldsymbol{q}}_k(t),\end{aligned} \tag{6}$$

where the superscripts "(C)" and "(A)" represent the contact patch coordinate system and absolute coordinate system, respectively. $\boldsymbol{A}^{(\mathrm{C})}$ is the transfer matrix between the absolute coordinate system and contact patch coordinate system. $\dot{\boldsymbol{u}}_{\mathrm{R}(x,y,\phi)}^{\mathrm{A}}$ is the velocity of wheel/rail contact point related to the rigid vibrations of the locomotive wheelset [37], and $\dot{\boldsymbol{u}}_{\mathrm{con}(x,y,\phi)}^{\mathrm{F}}$ is the velocity of wheel tread caused by the flexible vibrations of the locomotive wheelset. N_{fw} is the number of flexible modes of locomotive wheelset. $\boldsymbol{\Psi}_{\mathrm{fw}k}(\boldsymbol{x}_{\mathrm{con}})$ is the kth modal shape function of the locomotive wheelset, where the vector $\boldsymbol{x}_{\mathrm{con}}$ is the spatial position of wheel/rail contact point. $\boldsymbol{q}_k(t)$ is the kth generalized modal coordinate. Note that, the flexible vibrations of wheel tread of the locomotive wheelset are perceived as 0 when the wheelset flexibility is not considered (in Model-I and Model-III).

To usefully enhance the analytical precision of wheel/rail adhesion-slip contact and the resulted wheel tread

wear, in this study, the MKP-Yaw model [42] and FaStrip-MKP-Yaw model [31, 43] are applied for wheel/rail normal and tangential interactions, respectively. Moreover, the changing wheel/rail friction conditions which contribute greatly to wheel/rail frictional contact and wear are not considered hereon [31, 42], and only dry conditions are addressed in this work.

2.3 Long-Term Wheel Polygonal Wear Prediction Model

The USFD wear model which developed by University of Sheffield and KTH wear model based on Archard wear theory are the two mainly used methods on wheel/rail wear prediction [36, 44, 45]. Hereon, the USFD wear model is used for the long-term polygonal wear prediction of locomotive wheels.

By applying the FaStrip-MKP-Yaw model, the wear index distributions within the non-Hertzian contact patch can be deduced as [43, 46]

$$I_{\mathrm{w}}(\xi,\zeta)=\begin{cases}0, & \forall(\xi,\zeta)\in C_a,\\ q_x^{(s)}(\xi,\zeta)\cdot\gamma_x^{(s)}(\xi,\zeta)+q_y^{(s)}(\xi,\zeta)\cdot\gamma_y^{(s)}(\xi,\zeta), & \forall(\xi,\zeta)\in C_s,\end{cases} \tag{7}$$

with the tangential stress distributions given as

$$q_{(x,y)}^{(s)}(\xi,\zeta)=\frac{q_{(x,y)f}(\xi,\zeta)}{\sqrt{q_{xf}^2(\xi,\zeta)+q_{yf}^2(\xi,\zeta)}}\frac{\mu p_0(\zeta)}{a(\zeta)}\sqrt{a^2(\zeta)-(x-x_0(\zeta))^2}, \tag{8}$$

and relative slipping distributions given as

$$\begin{cases}\gamma_x^{(s)}(\xi,\zeta)=\vartheta_x-\zeta\vartheta_\phi+c_x\dfrac{\mu p_0(\zeta)}{Ga(\zeta)}\left[\dfrac{(\xi-x_0(\zeta))q_{xf}(\xi,\zeta)}{\sqrt{q_{xf}^2(\xi,\zeta)+q_{yf}^2(\xi,\zeta)}}\right.\\ \left.-\kappa'\left((\xi-x_0(\zeta)-d(\zeta))+\sqrt{(\xi-x_0(\zeta)-d(\zeta))^2-(a(\zeta)-d(\zeta))^2}\right)\right],\\ \gamma_y^{(s)}(\xi,\zeta)=\vartheta_y+\xi\vartheta_\phi+c_y\dfrac{\mu p_0(\zeta)}{Ga(\zeta)}\left[\dfrac{(\xi-x_0(\zeta))q_{yf}(\xi,\zeta)}{\sqrt{q_{xf}^2(\xi,\zeta)+q_{yf}^2(\xi,\zeta)}}\right.\\ \left.-\lambda'\left((\xi-x_0(\zeta)-d(\zeta))+\sqrt{(\xi-x_0(\zeta)-d(\zeta))^2-(a(\zeta)-d(\zeta))^2}\right)\right],\end{cases} \tag{9}$$

where the symbols C_a and C_s are wheel/rail adhesion region and slip region, respectively. $q_{(x,y)f}(\xi, \zeta)$ is the shear stresses obtained by the Fastsim algorithm, where the subscript "(x, y)" is the direction. ϑ_x, ϑ_y and ϑ_ϕ are the wheel/rail longitudinal, lateral and spinning creepage, respectively. G is the shear modulus. μ is the wheel/rail friction coefficient. $p_0(\zeta)$ is the normal pressure on the main axis of wheel/rail normal distance. $a(y)$ is the longitudinal distance between leading or rear edges of wheel/rail non-elliptic contact patch and main axis of the normal distance. Moreover, the symbols κ, κ', λ and λ' used in the above equations can be referred to Refs. [31, 46].

The updating process of wheel polygonal wear can be expressed as

$$\begin{aligned}&\{r_{\mathrm{w}},\boldsymbol{P}_{\mathrm{w}}(r_{\mathrm{w}})\}^{(N)}-\left\{r_{\mathrm{w}},k\cdot\Upsilon[\boldsymbol{w}(r_{\mathrm{w}})]\right\}^{(N+1)}\\ &\quad\Rightarrow\{r_{\mathrm{w}},\boldsymbol{P}_{\mathrm{w}}(r_{\mathrm{w}})\}^{(N+1)},\end{aligned} \tag{10}$$

with the wear amount at each discrete point of the wheel circumference after mth wheel revolution given as [24, 25]

$$\begin{aligned}\boldsymbol{w}(r_{\mathrm{w}})&=\sum_{i=1}^{m}\max\left[W(r_{\mathrm{w}},\zeta)\right]\\&=\sum_{i=1}^{m}\max\left[\int_{x_0(\zeta)-a(\zeta)}^{x_0(\zeta)+a(\zeta)}w_i(r_{\mathrm{w}},\xi,\zeta)\mathrm{d}\xi\right],\end{aligned} \tag{11}$$

where r_{w} denotes the circumferential position of the wheel. $\boldsymbol{w}_i(r_{\mathrm{w}}, \xi, \zeta)$ is the wear distributions in the wheel/rail contact patch [31]. The superscript "N" denotes the iteration number of polygonal wear evolution. k is the scaling coefficient of the predicted wheel polygonal wear corresponding to a certain operating distance and can shorten calculation time. Furthermore, $\Upsilon(\cdot)$ stands for moving smoothing method which is applied to smooth the calculated wheel circumferential irregularities after

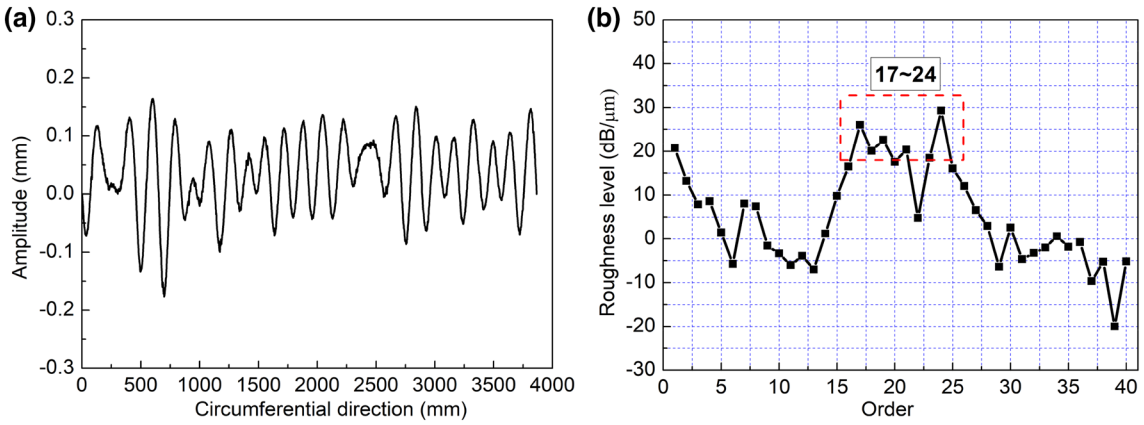

Figure 5 Wheel polygonal wear described in (**a**) orthogonal coordinate and (**b**) its roughness level analyzed in harmonic orders [31]

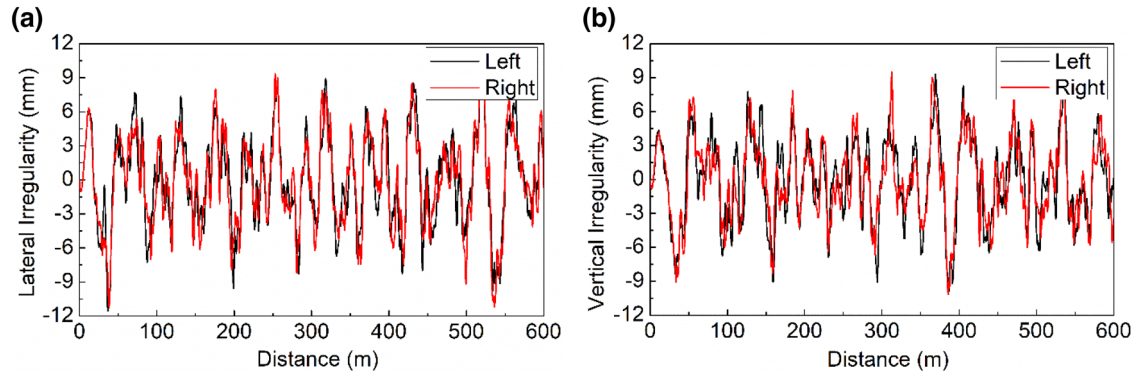

Figure 6 Track long-wave random irregularity: (**a**) Left- and (**b**) right-side

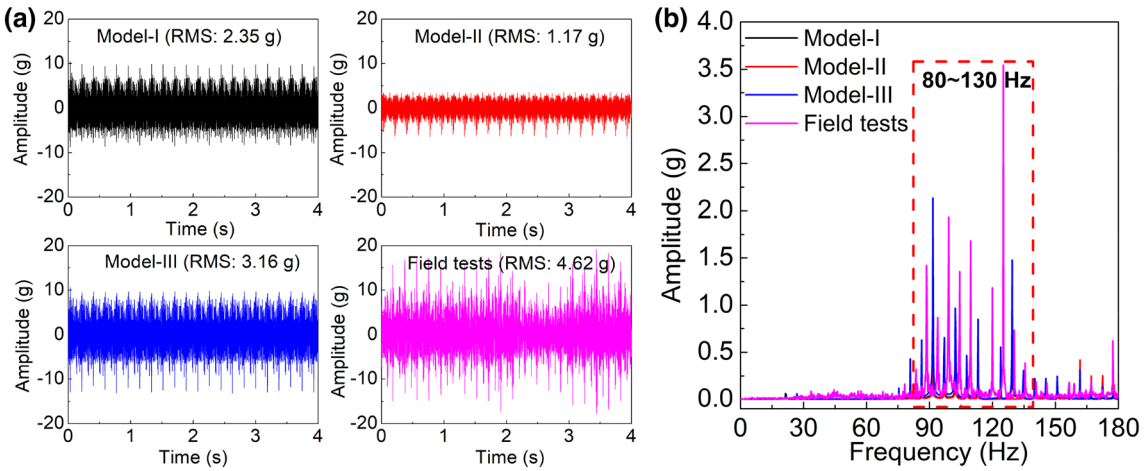

Figure 7 Effect of wheel/rail flexibility on the vertical vibration accelerations of locomotive wheelset displayed in (**a**) time domain and (**b**) frequency domain

each iteration simulation and can get rid of the short-wave irregularities and avoid the resulted high-frequency wheel/rail impacting contact [47].

3 Simulation Results

3.1 Effect of Wheel/Rail Flexibility on Its Interactions

The effect of wheel/rail flexibility on its interactions under the excitation of high-order wheel polygonal wear is numerically assessed hereon. The severe wheel polygonal wear with obvious 17th–24th harmonic orders is displayed in Figure 5 and considered in this simulation. Furthermore, the following background conditions are considered in the simulation:

- **Heavy-haul train**: The heavy-haul train travels on the track with a constant running velocity of 75 km/h, in which the traction or braking loadings are not implemented. Furthermore, the wheel circumference is 3.927 m, and the wheel/rail friction coefficient is set to be 0.55.
- **Track**: The ballast track is supposed to be straight, and the long-wave random irregularity (American Federal Railroad Administration Class 5 track irregularities, see Figure 6) is considered, and the rail cant is set to be 1/40.

The effect of wheel/rail flexibility on the vertical vibrations of locomotive wheelset with the excitation of wheel

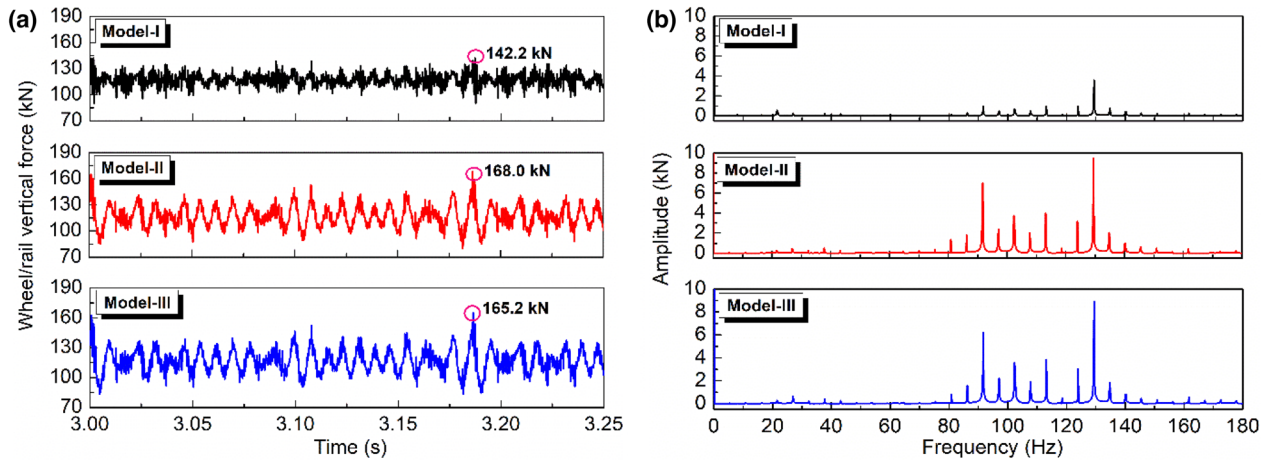

Figure 8 Comparison of wheel/rail vertical force subjected to different flexible modeling of the wheel/rail coupled system, displayed in (**a**) time domain and (**b**) frequency domain

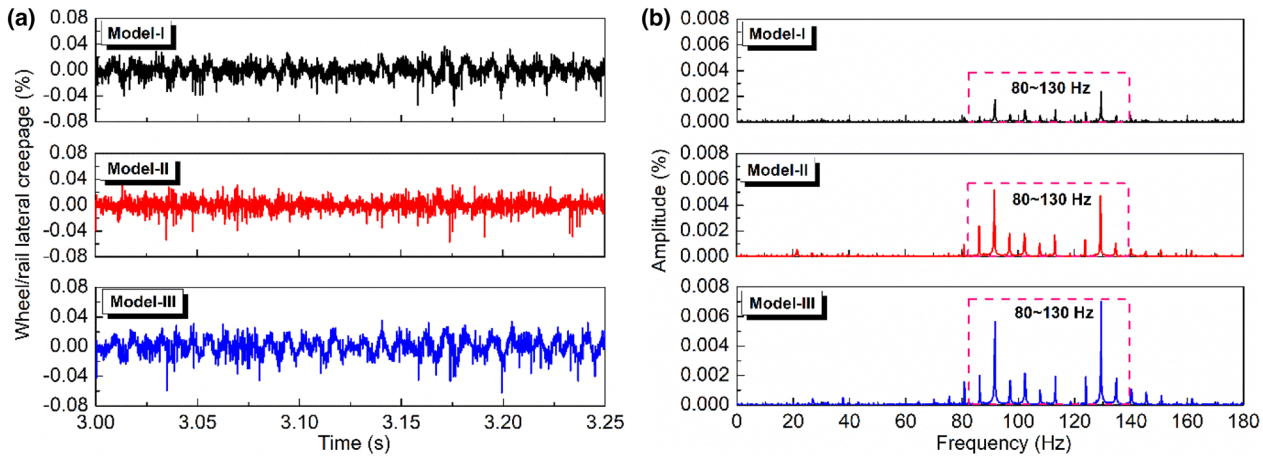

Figure 9 Comparison of wheel/rail lateral creepage subjected to different flexible modeling of the wheel/rail coupled system, displayed in (**a**) time domain and (**b**) frequency domain

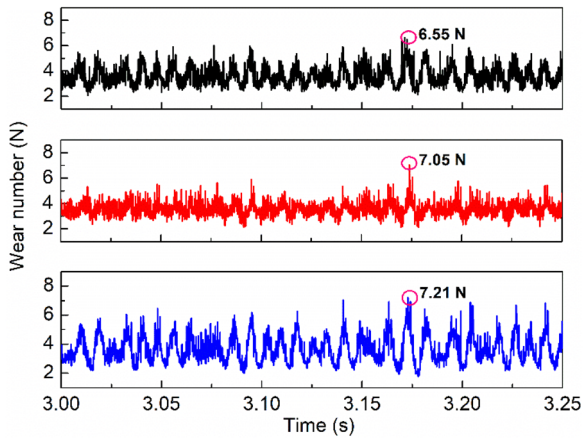

Figure 10 Wheel/rail wear number subjected to different flexible modeling of the wheel/rail coupled system

polygonal wear is demonstrated in Figure 7, where the simulation results obtained from the performed numerical models and field tests are compared in both time domain and frequency domain. It can be indicated that the severe 17th–24th order wheel polygonal wear can exacerbate the vibration behaviors of locomotive wheelsets with the striking response frequency range of 80–130 Hz. The vibration amplitudes of the wheelset obtained by Model-I and Model-III are significantly higher than that to Model-II, which is due to the resonance phenomenon resulted by the excitation frequency of wheel polygonal wear being close to the mode frequency of the locomotive wheelset with consideration of its flexibility. On the other hand, the vibration characteristics with respect to Model-III are closer to the field tests compared to that to Model-I and Model-II, especially within the frequency range of 80–130 Hz. Therefore, the vibration characteristics of locomotive unsprung components can be more accurately uncovered with consideration of the flexibility of locomotive wheelset and rails, especially for the medium- and high-frequency responses leaded by the flexible deformations of the wheelset and rails and short-wave corrugations.

The effect of wheel/rail flexibility on its rolling contact with the excitation of wheel polygonal wear, including wheel/rail vertical force and lateral creepage, is displayed in Figures 8 and 9. It is found that the 17th–24th order wheel polygonal wear can violently arise both vertical and tangential wheel/rail interactions. The wheel/rail flexibility contributes greatly to wheel/rail interactions. On one hand, the wheel/rail vertical interactions solved by Model-II and Model-III are more intense than that by Model-I, especially within the frequency range of 80–130 Hz. It is indicated that the flexibility of the rail plays a more important role in wheel/rail vertical interactions than that of the wheelset. On the other hand, the wheel/rail lateral creepage which can accelerate wheel/rail tread wear obtained by Model-I and Model-III fluctuate more significantly than that by Model-II. It is further revealed that the flexible deformations of the wheelsets and rails dominate in wheel/rail vertical and tangential interactions respectively, and the wheel/rail frictional interactions may be underestimated when the flexibility of the wheelset or rails is ignored. Furthermore, the spectral response with frequency range of 25–50 Hz can be found in wheel/rail vertical interactions (see Figure 8), which may be due to the 7th–8th order polygon wear and the excitations of discrete sleeper support.

The effect of wheel/rail flexibility on wheel/rail wear number which can be obtained as follows is displayed in Figure 10.

$$W = \iint_C \left(\left|q_x(\xi,\zeta)\cdot s_x(\xi,\zeta)\right| + \left|q_y(\xi,\zeta)\cdot s_y(\xi,\zeta)\right|\right)\mathrm{d}\xi\,\mathrm{d}\zeta, \tag{12}$$

with the relative slipping given as

$$\begin{cases} s_x(\xi,\zeta) = \vartheta_x - \zeta\vartheta_\phi, \\ s_y(\xi,\zeta) = \vartheta_y + \xi\vartheta_\phi, \end{cases} \tag{13}$$

where $q_x(x, y)$ and $q_y(x, y)$ are the longitudinal and transverse shear stresses, respectively.

It is shown that the 17th–24th order wheel polygonal wear can result in the related frictional wear which is directly associated with the wheel/rail tangential interactions. The wheel wear depth solved by Model-II and Model-III is higher than that by Model-I, since which could be more affected by the lateral bending and torsional deformations of the rail that have a large effect on wheel/rail frictional contact. Furthermore, the corresponding fluctuations leaded by high-order wheel polygonization with consideration of rail flexibility are also more obvious than that without consideration of rail flexibility.

3.2 Effect of Wheel/Rail Flexibility on Polygonal Wear Evolution

The locomotive wheels that experience frequent and severe abnormal vibration occurrences are pointed out to suffer 16th–25th order polygonal wear, and in addition to this, 7th–8th order polygonal wear can also be detected on these abnormally vibrational wheels [7]. The influence of wheel/rail flexibility on the polygonal wear evolution of locomotive wheels is simulated here.

In Refs. [24, 25], it is proved that the local wheel defects can observably induce the coupled vibrations and resonance of wheel/rail system, and such a periodic impact will cause the locomotive wheel to undergo an oscillation

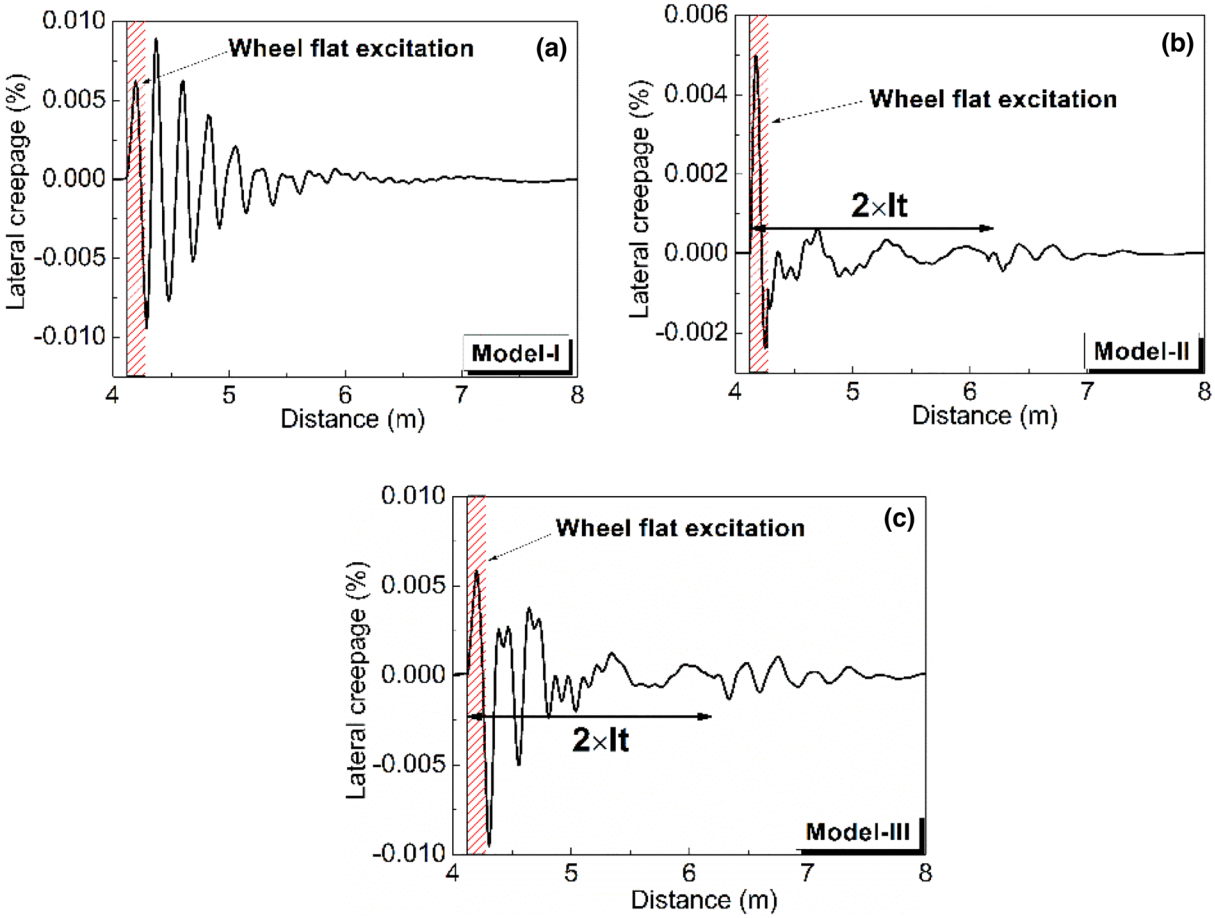

Figure 11 Wheel/rail lateral creepage subjected to different flexible modeling of the wheel/rail coupled system with the operating speed of 70 km/h: (**a**) Model-I, (**b**) Model-II and (**c**) Model-III

process. Simultaneously, the oscillations occurring on wheel/rail interface contribute to the according wheel/rail frictional interactions, and gradually, motivate the formation and development of the high-order wheel polygonal wear. Hereon, a wheel flat with the length of 0.15 m and depth of 0.1 mm is chosen as the raw wheel irregularity. Twenty iteration computations are carried out to exhibit the evolution mechanism of polygonal wear of locomotive wheels subjected to the wheel/rail flexibility. The traveling speeds within the range of 60–75 km/h are focused in wheel polygonal wear predictions since which occupy the majority in the heavy-haul locomotives' operations.

The wheel/rail lateral creepage due to the wheel flat which directly contribute to the formation of wheel polygon with the operating speed of 70 km/h is shown in Figure 11, and wheel/rail lateral creepage due to the wheel flat with other operating speeds is shown in Figure 12. It is seen that the wheel flat can excite the wheel/rail tangential contact in addition to the normal wheel/rail impact. The wheel/rail lateral creepage after the wheel flat is passed fluctuates relating to the wheel/rail coupled nonlinearity. The passing excitation frequency which corresponds to the low-order bending modes of the wheelset (with the mode frequencies of 81.0 Hz and 132.5 Hz) can be reproduced by using Model-I and Model-III when the flexibility of the wheelset is involved. On the other hand, the excitation frequency corresponding to the P2 resonance and the excitations of discrete sleeper support can be reflected by using Model-II and Model-III while the flexibility of the rails is involved. It is also interesting to find that the transmissions of the wheel/rail tangential interactions between the wheelsets of the same bogie are made through the rail and can be reflected only when the flexibility of the rail is considered (see the results obtained by Model-II and Model-III). Therefore, it is proved that the flexibility of both wheelset and rails plays a decisive role in wheel/rail frictional contact.

Figure 13 shows the influence of wheel/rail flexibility on polygonal wear evolution of locomotive wheels with

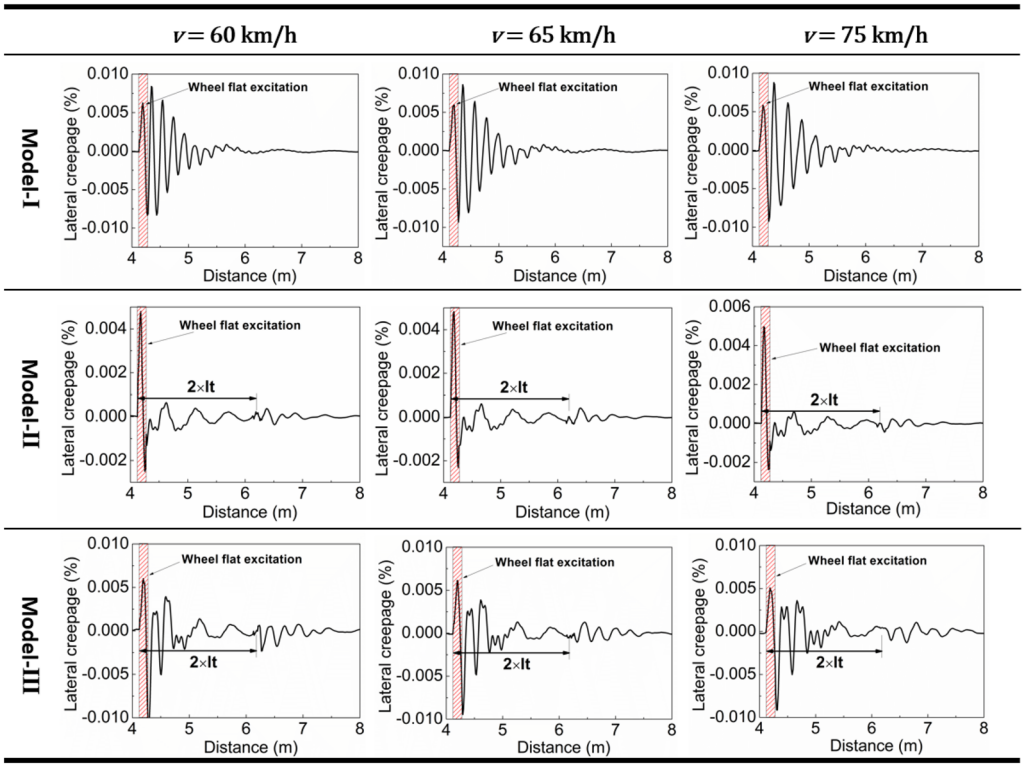

Figure 12 Wheel/rail lateral creepage subjected to different flexible modeling of the wheel/rail coupled system

a running speed of 70 km/h. The wheel polygonal wear is promoted to grow under the excitation of the wheel flat. It is noteworthy to find that the 16th–25th order polygonal wear evolves prominently when the wheelset flexibility is taken into account (Model-I and Model-III), which nevertheless, can't be reproduced with only consideration of the rail flexibility (Model-II). This high-order polygonal wear can result in prominent wheel/rail vertical interactions and vibrations on the unsprung components with the excitation frequency range of 76–124 Hz when a locomotive travels with a speed of 70 km/h and is testified to be induced by the low-order flexible modes of the locomotive wheelset (first bending mode of the wheelset with mode frequency of 81.0 Hz and lateral bending mode of wheel disc with mode frequency of 132.5 Hz, see Figure 4) according to the "fixed-frequency mechanism". Moreover, the 7th–8th order polygonal wear existing on locomotive wheels is associated with the excitation frequency range of 30–40 Hz and induced by P2 resonance or the excitations of discrete sleeper support, which can be reproduced by executing the numerical models with consideration of rail flexibility (Model-II and Model-III) and can't be reflected with only consideration of the wheelset flexibility (Model-I).

The effect of wheel/rail flexibility on polygonal wear evolution of locomotive wheels with other running speeds (including 60 km/h, 65 km/h and 75 km/h) is displayed in Figure 14. It is found that the traveling velocity also has a vital contribution to the evolution of the predominant polygonal wear of locomotive wheels. The predominant polygonization order decreases with the increase of the traveling velocity. Furthermore, the comparison results also prove that the low-order flexible modes of locomotive wheelset as well as the P2 resonance or the excitations of discrete sleeper support have the immediate responsibility for the development of the 16th–25th order and 7th–8th order wheel polygonal wear, respectively. It is further proved that the evolution of polygonal wear of locomotive wheels can be veritably simulated in the matter of the dominant orders of polygonal wear with consideration of the flexible effect of both wheelset and rails.

4 Countermeasures

4.1 Optimizing the Operation Strategy of Locomotives

Some publications mentioned that the optimizations of operation strategy of railway trains are conducive to the reduced development of wheel polygonal wear [11, 20]. Hereon, the effect of operation strategy of locomotives on the initiation and evolution of polygonal wear of locomotive wheels is evaluated based on detailed on-site investigations and statistics.

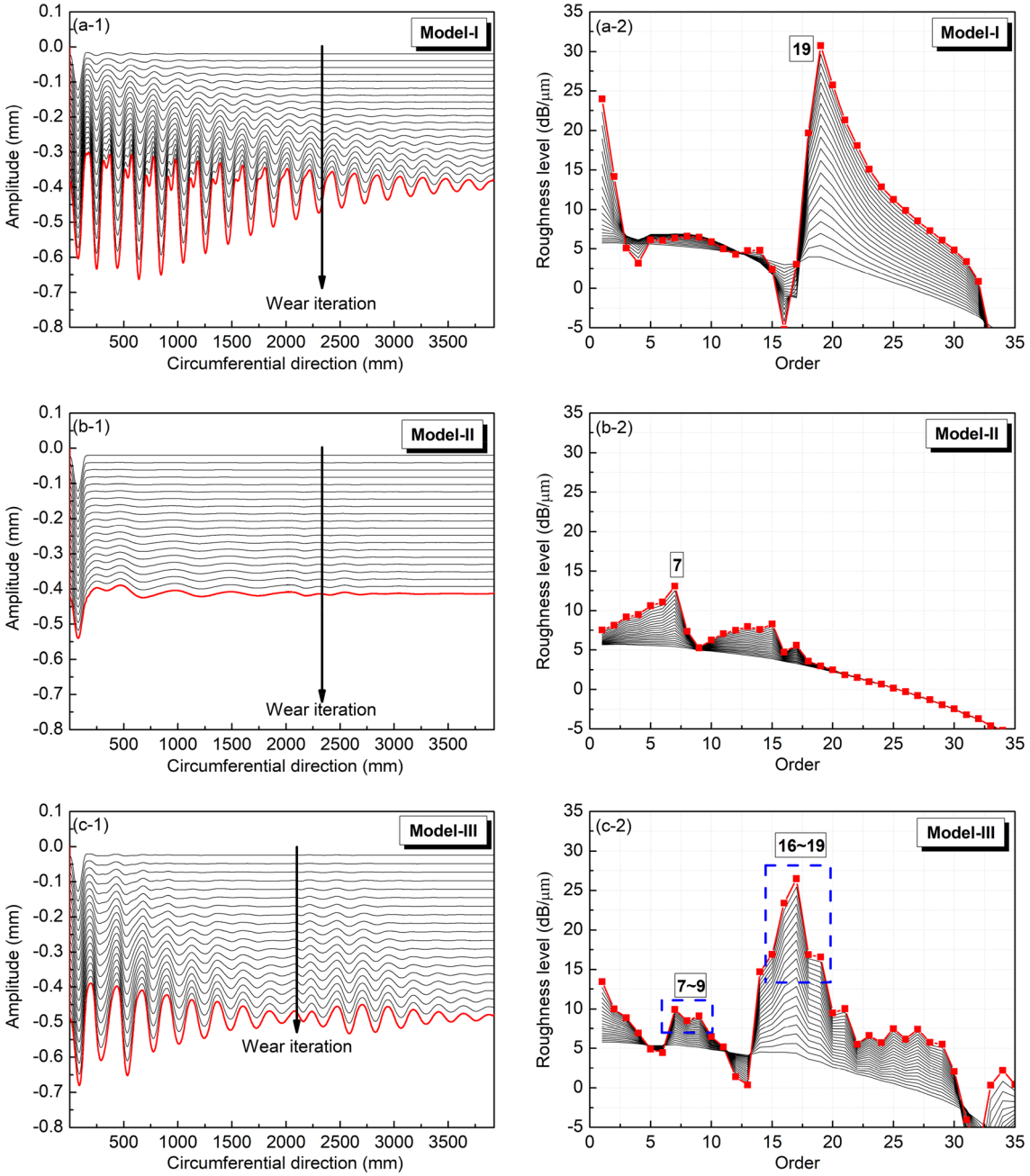

Figure 13 Effect of wheel/rail flexibility on polygonal wear evolution of locomotive wheels solved by (**a**) Model-I, (**b**) Model-II and (**c**) Model-III (the left and right diagrams are respectively described in orthogonal coordinate and harmonic order levels)

Two operation strategies of the locomotives, involving the single-line operation and mixed-line operation modes, are adopted in Depot YSQ in China. The locomotives belonging to Depot YSQ operate mostly on four lines, which are marked as Line ZY, Line ZW, Line ZP and Line ZL in this study. The operation strategies of the locomotives produced from the same manufacturer and with same structure designs and configurations in Depot YSQ were reorganized in June 2018. The Q-type under-floor wheel re-profiling lathe is mainly employed in Depot YSQ, which was reported to have defective effect on removing the high-order polygonal wear [7, 8]. The operation conditions of these locomotives are counted in Table 1.

It is suggested that the alarmed events of locomotives are not related to the production batch, nevertheless, to the operation strategies. The locomotives with 'T-1'

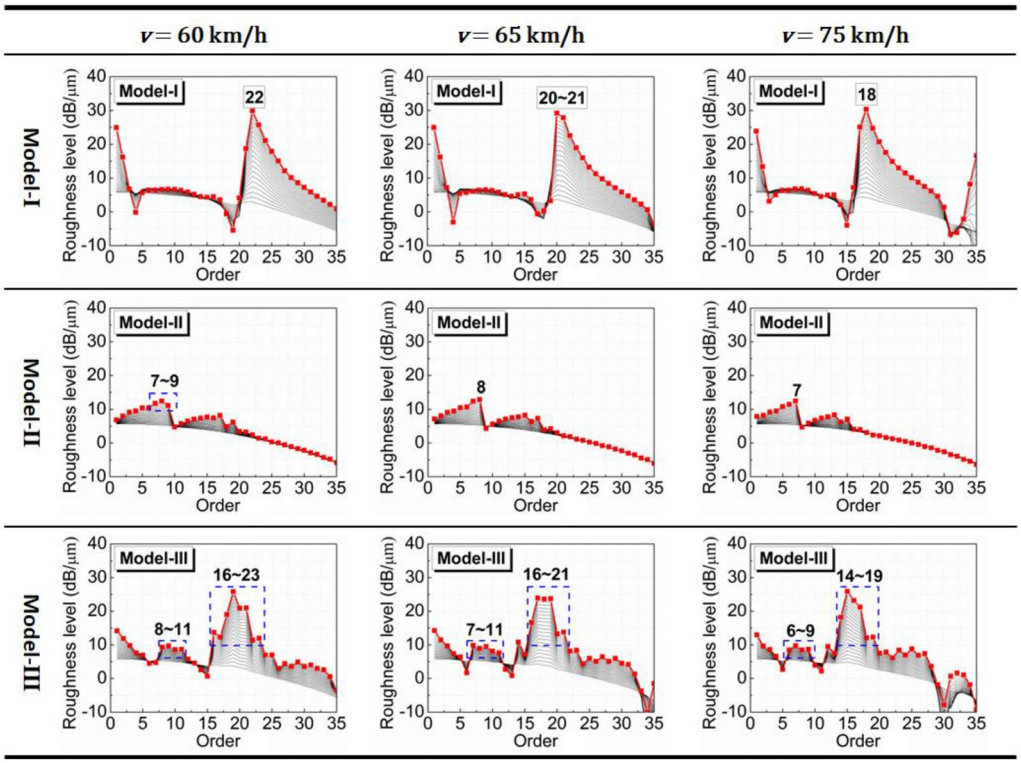

Figure 14 Effect of wheel/rail flexibility on polygonal wear evolution of locomotive wheels with different traveling speeds

operation strategy before operation adjustment have never suffered from the abnormal vibration alarm that induced by the high-order polygonal wear. However, the entire locomotives that traveled only on Line ZY (marked as 'T-2') underwent frequent abnormal vibration alarm events, and the wheels of which experienced inextirpable polygonal wear problems before and after operation adjustment despite with frequent re-profiling work. It is further pointed out that the initiation and evolution of wheel polygonal wear are highly corresponding to the situation that the locomotives operated purely on one regular line. Furthermore, the operation adjustment of the locomotives with 'T-2' operation strategy has totally no elimination effect on the polygonal wear and abnormal vibration issues.

To acquire a better understanding of the relationship between locomotive operation strategies and wheel polygonal wear development, the essential information of the four lines is given hereon. The statistical results of the track length with different slope and curve radius of the four lines are displayed in Figures 15 and 16, respectively. The total line length of Line ZY is greatly higher than that of the other three lines (748.954 km). It can be seen that the length of the line with large curve radius and small slope and corresponding proportion of Line ZY is significantly higher than that of the other three lines, in which

Table 1 Operation condition statistics of the in-service locomotives in Depot YSQ

Locomotive batch	Number	Before operation adjustment		After operation adjustment	
		Operation strategy	Number of alarmed locomotives	Operation strategy	Number of alarmed locomotives
A-1	74	T-1	0	T-3	0
B-1	7	T-1	0	T-3	0
B-2	8	T-1	0	T-1	0
B-3	23	T-2	23	T-3	23

Description: The symbol 'T-1', 'T-2' and 'T-3' employed for the operation conditions represent the scenario that the locomotives run on all lines except for Line ZY, the scenario that the locomotives run only on Line ZY, and the scenario that the locomotives run on all four lines, respectively

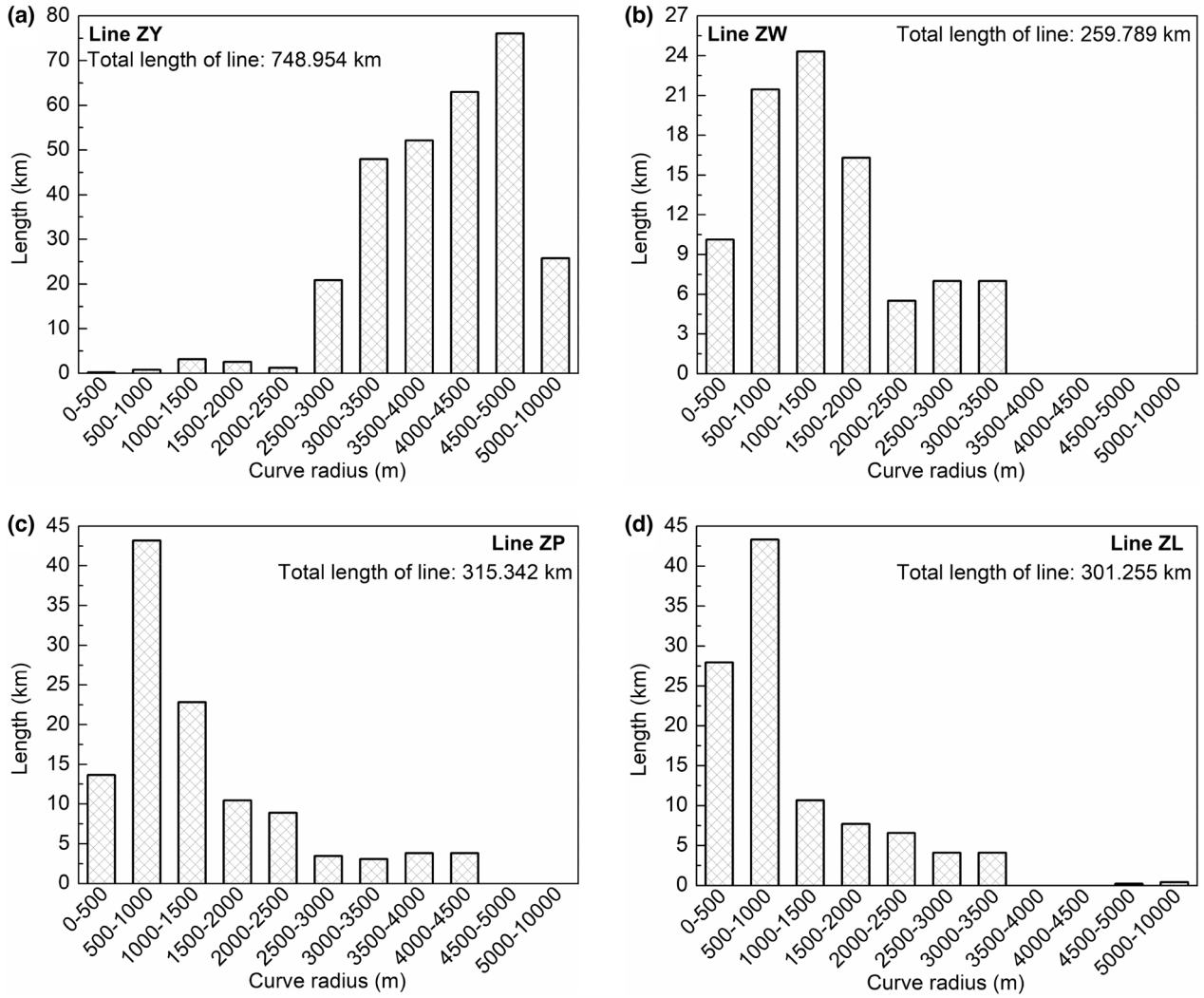

Figure 15 Statistical results of the curve radius and length of different in-service lines: (**a**) Line ZY, (**b**) Line ZW, (**c**) Line ZP and (**d**) Line ZL

the lines with the curve radius range of 4000–5000 m and with the slope range of – 2‰ to 2 ‰ account for the major components. The lines with the curve radius range of 0–1000 m and with shape slope, by contrast, occupy the major components of the other three lines. Therefore, the operating conditions of Line ZW, Line ZP and Line ZL are much more complicated than that of Line ZY, and the running speed of the locomotives on Line ZW, Line ZP and Line ZL is therefore limited and lower compared to that on Line ZY.

The maximum traveling speed of the locomotives in Depot YSQ is approximately 76 km/h. The statistical results of the durations with respect to different velocities and the entire durations within the velocity range of 65–76 km/h are counted in Figure 17. It is seen that the duration is largest when the locomotives travel within the speed range of 71–76 km/h on all four lines. The duration related to the speed range of 65–76 km/h of Line ZY is obviously higher than that of the other three lines (9.0 h), which may be due to the reason that the lines with small curve radius and large slope and according proportion of Line ZY are relatedly less than the other three lines.

The statistical results of mean values of the polygonal wear harmonic order levels of locomotive wheels with different batches and operation strategies are shown in Figure 18, where the locomotive wheels of 'A1', 'B2' and 'B3' batches are measured and counted. It is interesting to detect that the noteworthy 16th–19th and 24th order polygonal wear which result in the serious abnormal vibration phenomena dominate on the locomotive wheels in 'B3' batch, and 8th order polygonal wear can be also found on these wheels. On the other hand, only low-order polygonal wear can be found in the locomotive

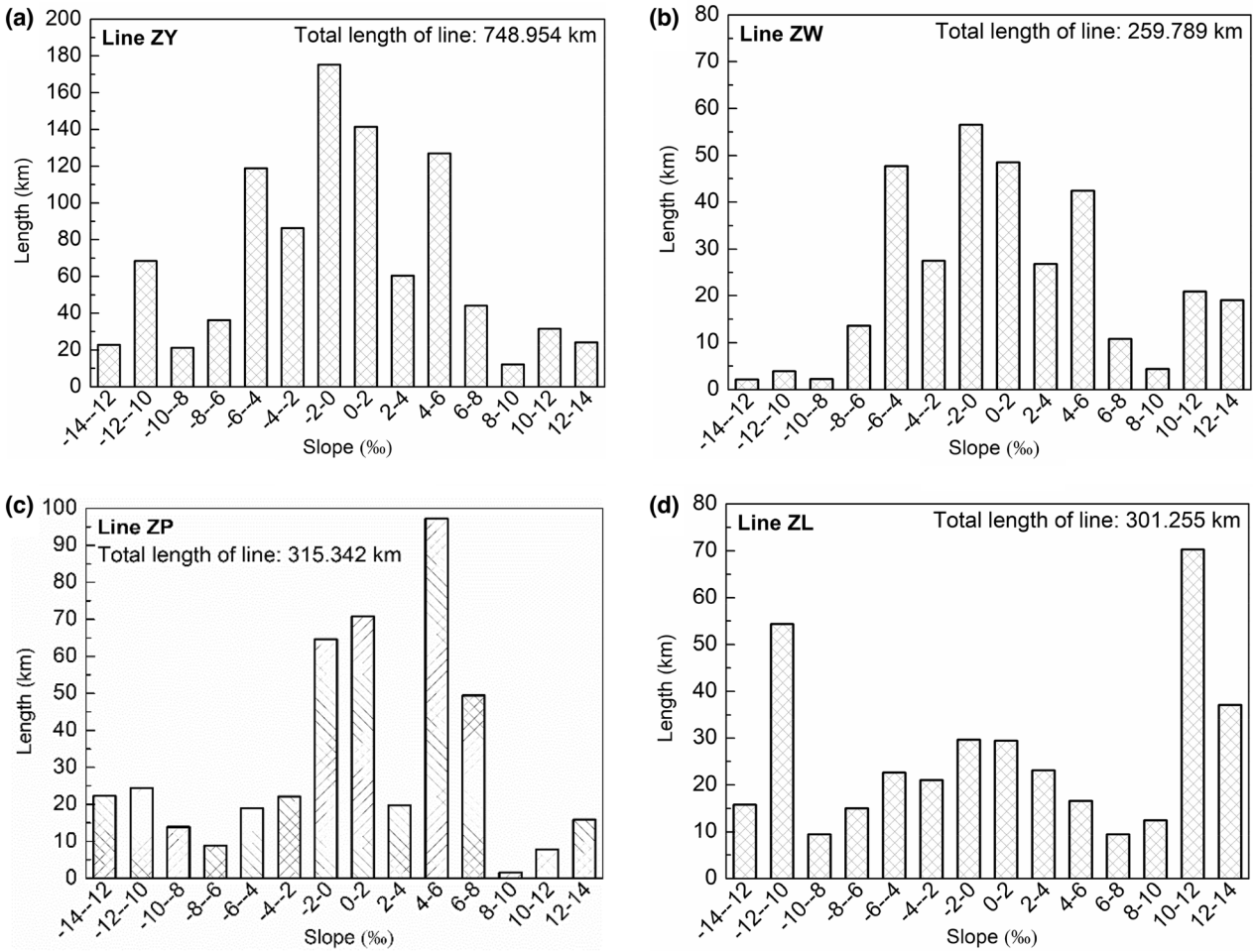

Figure 16 Statistical results of the ramp slope and length of different in-service lines: (**a**) Line ZY, (**b**) Line ZW, (**c**) Line ZP and (**d**) Line ZL

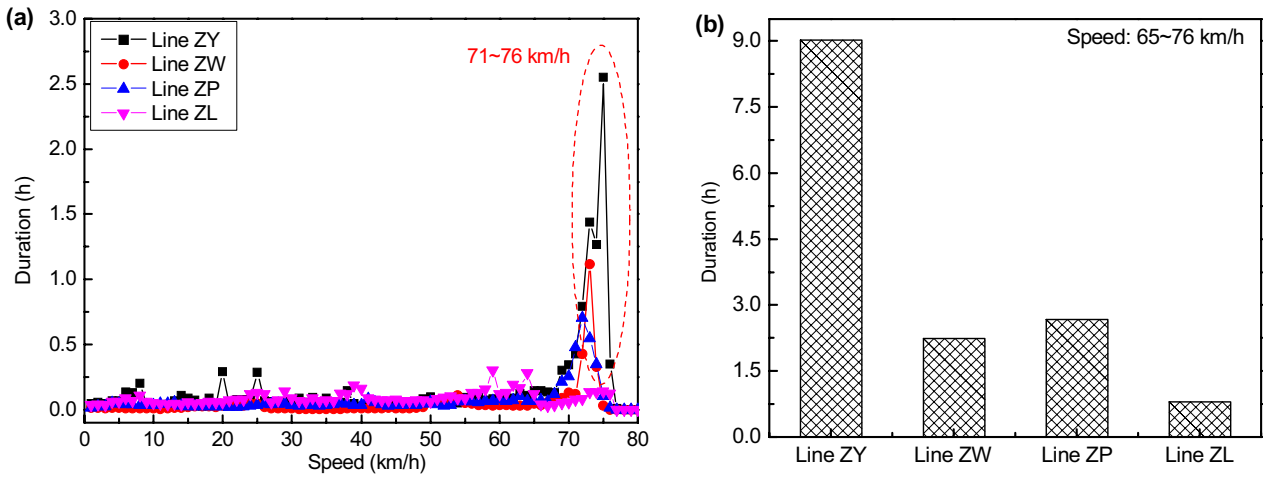

Figure 17 Statistical results of the durations of different in-service lines: (**a**) Duration related to different velocities and (**b**) duration within the velocity range of 65–80 km/h

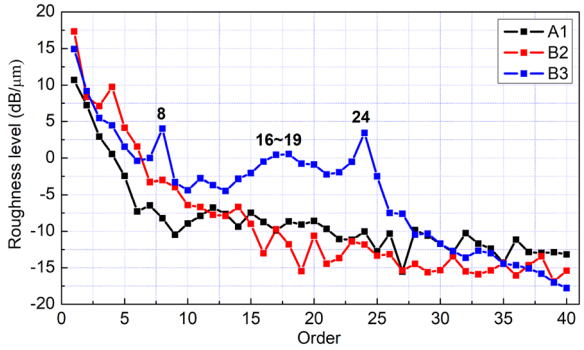

Figure 18 Statistical results of the polygonal wear of locomotive wheels with different batches and operation strategies

Table 2 Basic information of the tested three locomotive wheels

	Number of cuts	Operation mileage since the last re-profile (km)		
		Test before re-profiling	First test after re-profiling	Second test after re-profiling
Wheel A	One	44000	19000	65000
Wheel B	At least two	40000	24000	56000

wheels of 'A1' and 'B2' batches, and there were hardly any abnormal vibration alarm events took place on these locomotives. It is therefore suggested that the executions of mixed-line operation of locomotives can effectively avoid the initiation of wheel polygonal wear.

4.2 Enhancing the Quality of Wheel Re-profiling

The G-type under-floor wheel lathe has been most commonly applied to re-profile the damaged locomotive wheels aside from the Q-type one in China, which has also been proved demonstrating superior performances in comparison to the latter [7, 8]. The essential characteristics of these two types of under-floor wheel lathes have been introduced in Refs. [7, 8]. In this study, the influence of the re-profiling modes of the under-floor wheel lathe, namely the number of re-profiling cuts, on the elimination and development of polygonal wear of locomotive wheels is investigated through the tracking tests of wheel polygonal wear during an interval of the neighboring wheel re-profiling periods.

The tracking measurements of polygonal wear were conducted on two locomotive wheels that re-profiled with different number of re-profiling cuts during an interval of the neighboring wheel re-profiling periods. These two locomotive wheels suffered from continuingly serious abnormal vibration phenomena before wheel re-profiling, which are named as Wheel A and Wheel B hereon. The basic information of the three locomotive wheels is listed in Table 2.

The tracking testing results of the polygonal wear of locomotive wheels re-profiled with different number of re-profiling cuts are displayed in Figure 19. The high-order polygonal wear can be better removed by the G-type under-floor wheel lathe with a firmer wheelset fastening compared to that by the Q-type under-floor wheel lathe after wheel re-profiling. It is seen that the development of the 16th–20th order polygonal wear after an operation mileage of 46000 km is very obvious with only one cut (with the roughness level of 25 dB/μm). By contrast, the high-order polygonal wear can be availably eliminated with at least two cuts, and it developed much more slowly after wheel re-profiling. It is indicated that the high-order polygonal wear of the locomotive wheels develops slowly with a sound re-profiling method and the resulting polygonal wear with relatively lower roughness level after wheel re-profiling. But it is worth mentioning that the combinative application of under-floor wheel lathe and multi-cut wheel re-profiling can not only consume a lot of operating time and labor cost, but also aggrandize the material loss amount of locomotive wheels.

4.3 Discussion

4.3.1 On the Effect of Operation Strategy on the Initiation and Evolution of Polygonal Wear

The initiation of the severe wheel polygonal wear problems in Depot YSQ may be due to reason that the durations within the velocity range of 65–76 km/h when the locomotives operate on Line ZY is obviously larger than that on the other three lines, even though the line conditions of Line ZY is worse than that of other three lines. When the locomotives are traveling with the velocity range of 65–76 km/h, the passing frequency of this high-order polygonal wear is close to the coupled resonant frequency of the wheel/rail system, and the excitations of the wheel/rail coupled resonance and wheel/rail flexible interactions contribute to the initiation of 16th–25th order polygonal wear of locomotive wheels.

Further numerical investigations on the relation between the operation strategy of railway trains, traveling velocities, line conditions as well as initiation and evolution of wheel polygonal wear of should be conducted, which have been rarely discussed in the past.

4.3.2 On the Effect of Wheel Re-profiling on the Evolution of Polygonal Wear

The second testing results of polygonal wear of these two locomotive wheels after re-profiling are compared in Figure 20. It is further proved that re-profiling the polygonized wheels with at least two cuts can effectively

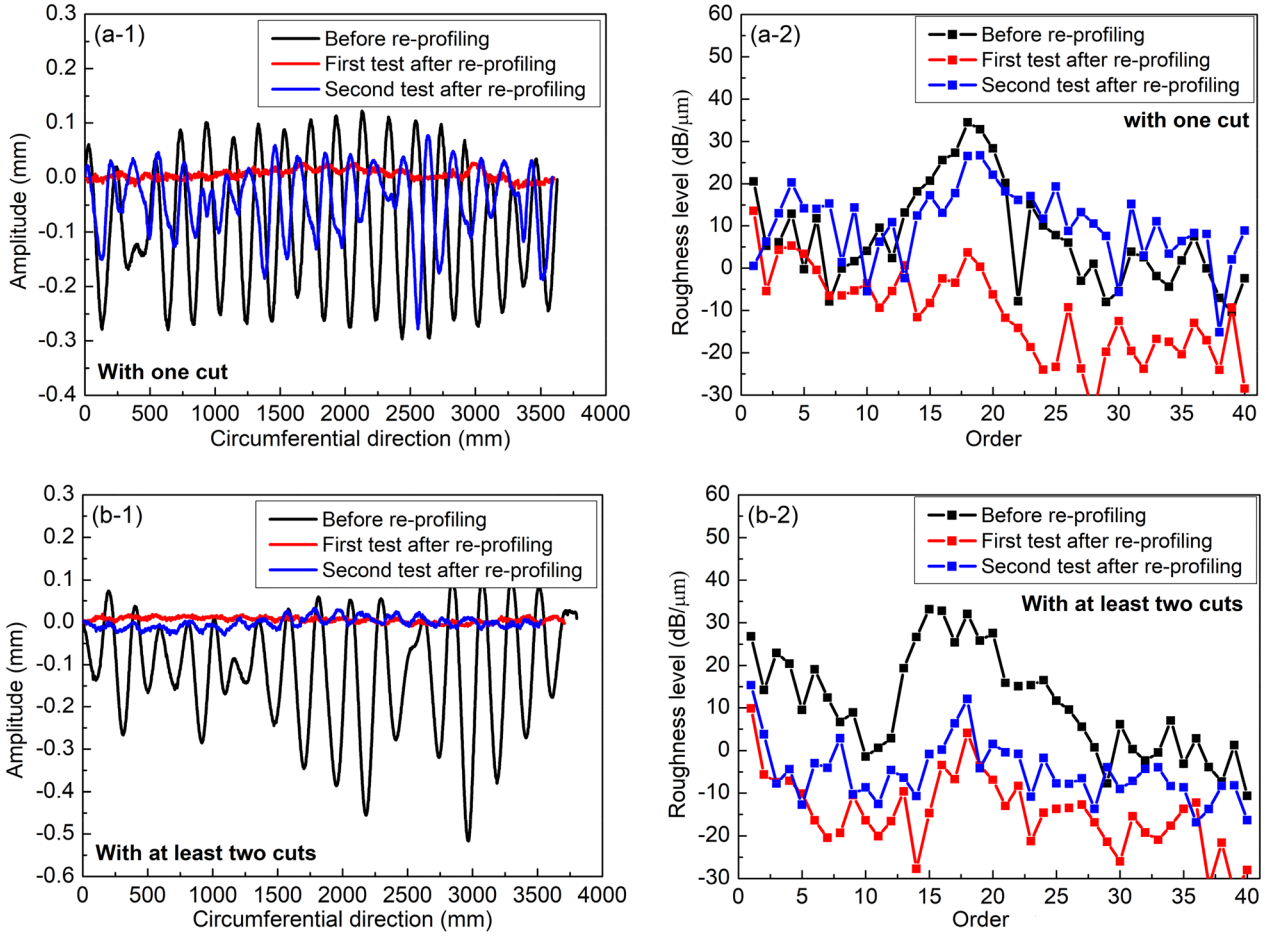

Figure 19 Tracking testing results of polygonal wear of locomotive wheels re-profiled with different number of re-profiling cuts: (**a**) Wheel A and (**b**) Wheel B

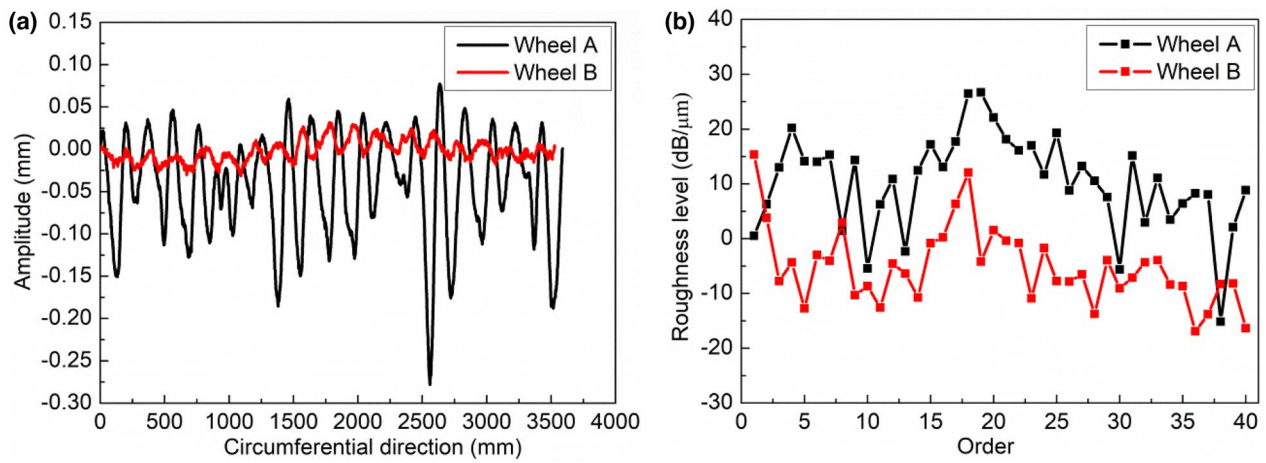

Figure 20 Comparison of the second testing results of wheel polygonal wear after re-profiling displayed in (**a**) orthogonal coordinate and (**b**) its roughness level analyzed in harmonic orders

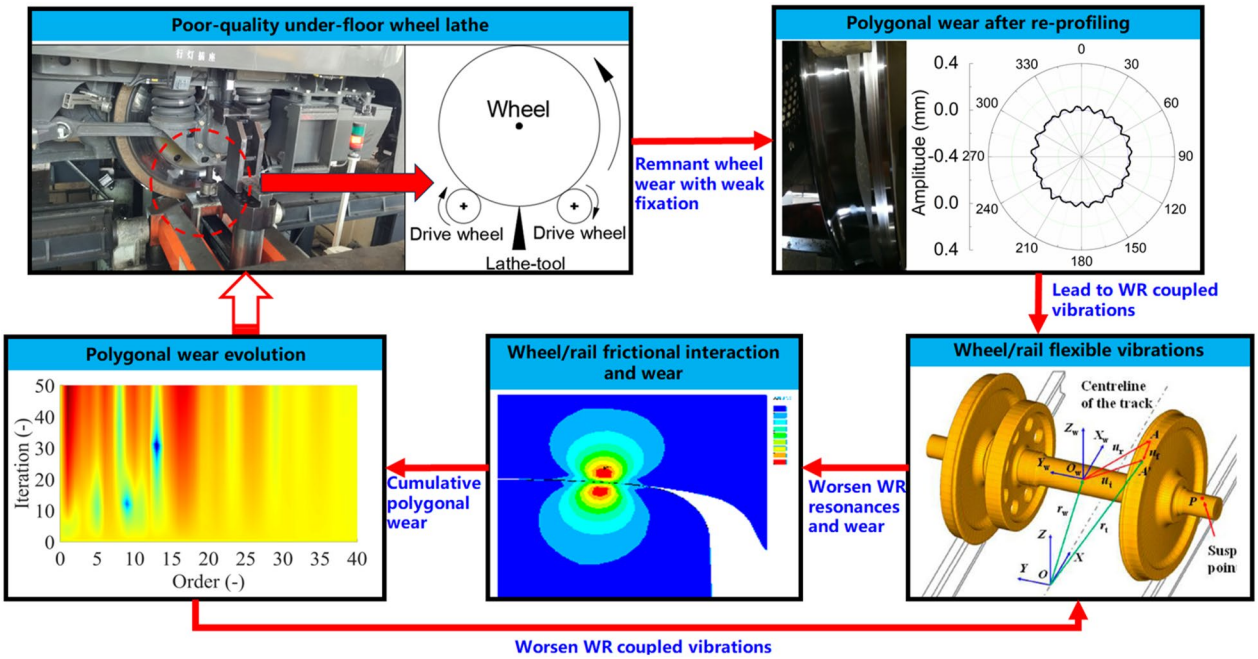

Figure 21 Deterioration process of wheel polygonal wear

get rid of the high-order polygonal wear with a larger cutting quantity.

It is exhibited that the number of re-profiling cuts affects not only the elimination but also the development of wheel polygonal wear after re-profiling. The residual high-order polygonal wear with the unsound re-profiling way can excite the wheel/rail coupled interactions corresponding to the natural modes of the wheel/rail system and intensify according wheel/rail frictional wear, and further, promote the development of the homologous high-order polygonal wear (see Figures 9 and 21). Therefore, the effective elimination of the high-order polygonal wear can hold back its development after wheel re-profiling.

5 Conclusions

The polygonal wear of railway wheels often results in impacting contact at wheel/rail interface and consistent shocks on train unsprung parts (such as axlebox, wheel axle, gear pair, motor cover), especially when the high-order components predominates on the non-circular wheels. In this work, the probabilities of the evolution of polygonal wear of locomotive wheels subjected to the wheel/rail flexibility are compared and determined by applying the long-term specific polygonal wear prediction models with consideration of different flexible modeling of the wheel/rail coupled system, which have rarely been discussed in the past. Furthermore, regarding the perniciousness of the polygonal wear, two countermeasures are proposed, and the availabilities of which are validated through the field investigations. The following conclusions can be drawn.

The severe wheel polygonal wear can deteriorate wheel/rail coupled vibrations and frictional interactions. The vibration performances of locomotive wheelset can be more truly simulated in time domain and frequency domain with consideration of the flexibility of both wheelset and rails. The flexible deformations of the rails have a relatively larger influence on the wheel/rail frictional wear compared to that of the wheelset under the excitation of wheel polygonal wear. On the other hand, based on the "fixed-frequency mechanism", the low-order bending modes of locomotive wheelset and P2 resonance or the excitations of discrete sleeper support are indicated to contribute predominantly to the formation and development of 16th–25th order and 7th–8th order polygonal wear of locomotive wheels, respectively. It is also proved that the evolution of polygonal wear of locomotive wheels can be more veritably reproduced with consideration of the flexible effect of both wheelset and rails.

Two countermeasures aiming for the abnormal wheel polygonization and its execrable impact on wheel/rail rolling contact are also came forward in this paper. Through the massive as well as tracking tests of

polygonal wear of locomotive wheels, the executions of mixed-line operation of locomotives, and adopting the under-floor wheel lathe with at least two cuts are proved to be capable of effectively avoiding the initiation and rapid growth of the polygonal wear.

In the further, the extraordinary relationship between the evolution of wheel polygonal wear and specific line conditions occurred in Depot YSQ will be examined by performing the long-term polygonal wear prediction simulations. On the other hand, more effective measures against the development of polygonal wear of locomotive wheelset should be proposed. Adopting the tread braking mode and ameliorating braking controlling logic may be a good option, and this is underway by the authors.

Acknowledgements
Not applicable.

Authors' Contributions
YY wrote the manuscript and did the analysis. FC and PL contributed to the field investigations and data arrangements. LL, KW and WZ revised the manuscript. All authors read and approved the final manuscript. All authors read and approved the final manuscript.

Funding
Supported by National Natural Science Foundation of China (Grant Nos. U2268210, 52302474, 52072249).

Availability of Data and Materials
The data that support the findings of this study are available from the corresponding author upon reasonable request.

Declarations

Competing interests
The authors declare no competing financial interests.

Author Details
[1]State Key Laboratory of Mechanical Behavior and System Safety of Traffic Engineering Structures, Shijiazhuang Tiedao University, Shijiazhuang 050043, China. [2]State Key Laboratory of Rail Transit Vehicle System, Southwest Jiaotong University, Chengdu 610031, China.

Received: 25 June 2023 Revised: 31 October 2023 Accepted: 3 February 2024
Published online: 29 February 2024

References

[1] W M Zhai, X S Jin, Z F Wen, et al. Wear problems of high-speed wheel/rail systems: Observations, causes, and countermeasures in China. *Applied Mechanics Reviews*, 2020, 72(6): 060801.
[2] Y F Yang, L Ling, C Wang, et al. Wheel/rail dynamic interaction induced by polygonal wear of locomotive wheels. *Vehicle System Dynamics*, 2022, 60(1): 211-235.
[3] P F Liu, S P Yang, Y Q Liu. Full-scale test and numerical simulation of wheelset-gear box vibration excited by wheel polygon wear and track irregularity. *Mechanical Systems and Signal Processing*, 2022, 167:108515.
[4] H Wu, P B Wu, F S Li, et al. Fatigue analysis of the gearbox housing in high-speed trains under wheel polygonization using a multibody dynamics algorithm. *Engineering Failure Analysis*, 2019, 100: 351-364.
[5] Y G Ye, B Zhu, P Huang, et al. OORNet: A deep learning model for on-board condition monitoring and fault diagnosis of out-of-round wheels of high-speed trains. *Measurement*, 2022, 199: 111268.
[6] G Q Tao, Z F Wen, X S Jin, et al. Polygonisation of railway wheels: A critical review. *Railway Engineering Science*, 2020, 28(4): 317-345.
[7] Y F Yang, L Ling, P F Liu, et al. Experimental investigation of essential feature of polygonal wear of locomotive wheels. *Measurement*, 2020, 166: 108199.
[8] G Q Tao, L F Wang, Z F Wen, et al. Measurement and assessment of out-of-round electric locomotive wheels. *Proceedings of the Institution of Mechanical Engineers, Part F: Journal of Rail and Rapid Transit*, 2018, 232(1): 275-287.
[9] J C O Nielsen, R Lundén, A Johansson. Train-track interaction and mechanisms of irregular wear on wheel and rail surfaces. *Vehicle System Dynamics*, 2003, 40(1-3): 3-54.
[10] W B Cai, X W Wu, M R Chi, et al. High-order wheel polygonal wear growth and mitigation: A parametric study. *Mechanical Systems and Signal Processing*, 2023, 186: 109917.
[11] Y Wu, X Du, J Han, et al. Experimental analysis of the mechanism of high-order polygonal wear of wheels of a high-speed train. *Journal of Zhejiang University-Science A*, 2017, 18(8): 579-592.
[12] Y Wu, J N Wang, M K Liu, et al. Polygonal wear mechanism of high-speed wheels based on full-size wheel-rail roller test rig. *Wear*, 2022, 494-495: 204234.
[13] S Qu, B Zhu, J Zeng, et al. Experimental investigation for wheel polygonisation of high-speed trains. *Vehicle System Dynamics*, 2021, 59(10): 1573-1586.
[14] C Z Ma, L Gao, R X Cui, et al. The initiation mechanism and distribution rule of wheel high-order polygonal wear on high-speed railway. *Engineering Failure Analysis*, 2021, 119: 104937.
[15] X Zhao, G X Chen, J Z Lyv, et al. Study on the mechanism for the wheel polygonal wear of high-speed trains in terms of the frictional self-excited vibration theory. *Wear*, 2019, 426-427: 1820-1827.
[16] B W Wu, Z Y Shang, J B Pan, et al. Analysis on the formation cause for the high-order wheel polygonization of the high-speed trains based on the finite element method. *Vehicle System Dynamics*, 2023, 61(1): 1-18.
[17] X S Jin, L Wu, J Y Fang, et al. An investigation into the mechanism of the polygonal wear of metro train wheels and its effect on the dynamic behaviour of a wheel/rail system. *Vehicle System Dynamics*, 2012, 50(12): 1817-1834.
[18] G Q Tao, C X Xie, H Y Wang, et al. An investigation into the mechanism of high-order polygonal wear of metro train wheels and its mitigation measures. *Vehicle System Dynamics*, 2021, 59(10): 1557-1572.
[19] G Q Tao, Z F Wen, X R Liang, et al. An investigation into the mechanism of the out-of- round wheels of metro train and its mitigation measures. *Vehicle System Dynamics*, 2019, 57(1): 1-16.
[20] B Fu, S Bruni, S H Luo. Study on wheel polygonization of a metro vehicle based on polygonal wear simulation. *Wear*, 2019, 438-439: 203071.
[21] R Fröhling, U Spangenberg, E Reitmann. Root cause analysis of locomotive wheel tread polygonization. *Wear*, 2019, 432-433: 102911.
[22] U Spangenberg. Variable frequency drive harmonics and interharmonics exciting axle torsional vibration resulting in railway wheel polygonization. *Vehicle System Dynamics*, 2020, 58(3): 404-424.
[23] G Q Tao, L F Wang, Z F Wen, et al. Experimental investigation into the mechanism of the polygonal wear of electric locomotive wheels. *Vehicle System Dynamics*, 2018, 56(6): 883-899.
[24] G Q Tao, Z F Wen, G S Chen, et al. Locomotive wheel polygonisation due to discrete irregularities: simulation and mechanism. *Vehicle System Dynamics*, 2021, 59(6): 872-889.
[25] Y G Ye, D C Shi, P Krause, et al. Wheel flat can cause or exacerbate wheel polygonization. *Vehicle System Dynamics*, 2020, 58(10): 1575-1604.
[26] B Peng, S Iwnicki, P Shackleton, et al. General conditions for railway wheel polygonal wear to evolve. *Vehicle System Dynamics*, 2021, 59(4): 568-587.
[27] D B Cui, B Y An, P Allen, et al. Effect of the turning characteristics of underfloor wheel lathes on the evolution of wheel polygonization. *Proceedings of the Institution of Mechanical Engineers, Part F: Journal of Rail and Rapid Transit*, 2019, 233(5): 479-488.
[28] G Q Tao, X L Liu, Z F Wen, et al. Formation process, key influencing factors, and countermeasures of high-order polygonal wear of locomotive wheels. *Journal of Zhejiang University-Science A*, 2021, 22(1): 70-84.

[29] W B Cai, M R Chi, X W Wu, et al. Experimental and numerical analysis of the polygonal wear of high-speed trains. *Wear*, 2019, 440-441: 203079.
[30] X W Wu, S Rakheja, W B Cai, et al. A study of formation of high order wheel polygonalization. *Wear*, 2019, 424-425: 1-14.
[31] Y F Yang, M K Xu, L Ling, et al. Polygonal wear evolution of locomotive wheels subjected to anti-slip control. *Wear*, 2022, 500-501: 204348.
[32] U Spangenberg, R Fröhling. Solving locomotive wheel polygonisation by reducing variable frequency drive interharmonics. *Proceedings of the Institution of Mechanical Engineers, Part F: Journal of Rail and Rapid Transit*, 2021, 235(1): 73-82.
[33] C Y Chang, G Li, Y H Zhang, et al. Experimental study on influence of wheel-rail material hardness matching on wheel polygonal wear. *China Railway Science*, 2018, 39(2): 87-93. (in Chinese)
[34] B Morys. Enlargement of out-of-round wheel profiles on high-speed trains. *Journal of Sound and Vibration*, 1999, 227(5): 965-978.
[35] A Johansson, C Andersson. Out-of-round railway wheels—a study of wheel polygonalization through simulation of three-dimensional wheel–rail interaction and wear. *Vehicle System Dynamics*, 2005, 43(8): 539-559.
[36] F Braghin, R Lewis, R S Dwyer-Joyce, et al. A mathematical model to predict railway wheel profile evolution due to wear. *Wear*, 2016, 261(11): 1253-1264.
[37] W M Zhai. *Vehicle-track coupled dynamics: Theory and applications*. Springer, Singapore, 2020.
[38] W M Zhai, K Y Wang, C B Cai. Fundamentals of vehicle-track coupled dynamics. *Vehicle System Dynamics*, 2009, 47(11): 1349-1376.
[39] Y F Yang, L Ling, Y F Yang, et al. Effects of wheelset flexibility on locomotive-track interaction due to rail weld irregularities. *Vehicle System Dynamics*, 2022, 60(9): 3088-3108.
[40] P Vila, L Baeza, J Martínez-Casas, et al. Rail corrugation growth accounting for the flexibility and rotation of the wheelset and the non-Hertzian and non-steady-state effects at contact patch. *Vehicle System Dynamics*, 2014, 52(S1): 92-108.
[41] L Baeza, J Giner-Navarro, D J Thompson, et al. Eulerian models of the rotating flexible wheelset for high frequency railway dynamics. *Journal of Sound and Vibration*, 2019, 449: 300-314.
[42] Y Sun, W M Zhai, Y G Ye, et al. A simplified model for solving wheel/rail non-Hertzian normal contact problem under the influence of yaw angle. *International Journal of Mechanical Sciences*, 2020, 174: 105554.
[43] Y F Yang, L Ling, J C Wang, et al. A numerical study on tread wear and fatigue damage of railway wheels subjected to anti-slip control. *Friction*, 2023, 11: 1470-1492.
[44] R Lewis, U Olofsson. *Wheel-rail interface handbook*. Woodhead Publishing Limited, Oxford, 2009.
[45] B Peng, S Iwnicki, P Shackleton, et al. Comparison of wear models for simulation of railway wheel polygonization. *Wear*, 2019, 436-437: 203010.
[46] M H Sichani, R Enblom, M Berg. A fast wheel/rail contact model for application to damage analysis in vehicle dynamics simulation. *Wear*, 2016, 366-367: 123-130.
[47] X X Yang, G Q Tao, W Li, et al. On the formation mechanism of high-order polygonal wear of metro train wheels: Experiment and simulation. *Engineering Failure Analysis*, 2021, 127: 105512.

Yunfan Yang born in 1992, is currently a lecturer at *State Key Laboratory of Mechanical Behavior and System Safety of Traffic Engineering Structures, Shijiazhuang Tiedao University, China*. He received his Ph.D degree from *State Key Laboratory of Traction Power, Southwest Jiaotong University, China*, in 2022. His research interests include wheel-rail wear evolution and train-track non-linear dynamics.

Feifan Chai born in 1998, is currently a master candidate at *State Key Laboratory of Rail Transit Vehicle System, Southwest Jiaotong University, China*. Her research interests include wheel-rail rolling contact.

Pengfei Liu born in 1986, is currently a professor at *State Key Laboratory of Mechanical Behavior and System Safety of Traffic Engineering Structures, Shijiazhuang Tiedao University, China*. He received his Ph.D degree from *State Key Laboratory of Traction Power, Southwest Jiaotong University, China*, in 2015. His research interests include railway vehicle dynamics and control.

Liang Ling born in 1986, is currently a professor at *State Key Laboratory of Rail Transit Vehicle System, Southwest Jiaotong University, China*. He received his PhD degree from *Southwest Jiaotong University, China*, in 2015. His research areas cover the railway vehicle-track coupled dynamics, wheel-rail contact mechanics and friction performance, and safety active control of railway vehicles.

Kaiyun Wang born in 1974, is currently a professor at *State Key Laboratory of Rail Transit Vehicle System, Southwest Jiaotong University, China*. He received his PhD degree from *Southwest Jiaotong University, China*, in 2013. His research interests include railway vehicle-track coupled dynamics, and safety control of railway vehicles.

Wanming Zhai born in 1963, is an academician of *Chinese Academy of Sciences, China*, and an international member of the *U.S. National Academy of Engineering (NAE), USA*. He received his Ph.D. degree in rail vehicle engineering in 1992 from *Southwest Jiaotong University, China*. Currently, he is a Chair Professor, the Dean of Faculty of Transportation Engineering, and the Chairman of Academic Committee of Southwest Jiaotong University, China. His research interest is mainly in railway engineering dynamics, especially in vehicle-track coupled dynamics and train-track-bridge dynamic interaction.